NUCLEAR DATA AND MEASUREMENTS SERIES

ANL/NDM-10
Cross Sections for (n,p) Reactions on ^{27}Al, ^{46,47,48}Ti, ^{54,56}Fe, ^{58}Ni, ^{59}Co, and ^{64}Zn from Near Threshold to 10 MeV

by

Donald L. Smith and James W. Meadows

January 1975

ARGONNE NATIONAL LABORATORY,
ARGONNE, ILLINOIS 60439, U.S.A.

NUCLEAR DATA AND MEASUREMENTS SERIES

ANL/NDM-10

Cross Sections for (n,p) Reactions on ^{27}Al, $^{46,47,48}Ti$, $^{54,56}Fe$, ^{58}Ni, ^{59}Co and ^{64}Zn from Near Threshold to 10 MeV

by

Donald L. Smith and James W. Meadows

January 1975

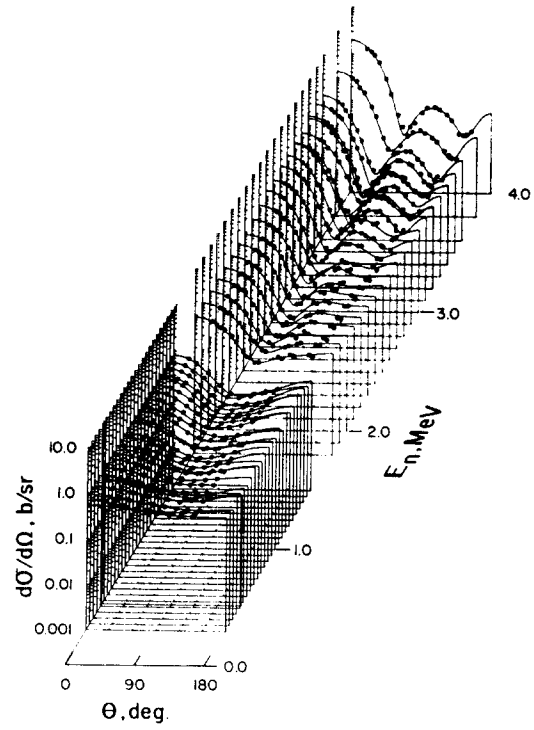

U of C - AUA - USAEC

ARGONNE NATIONAL LABORATORY,
ARGONNE, ILLINOIS 60439, U.S.A.

The facilities of Argonne National Laboratory are owned by the United States Government. Under the terms of a contract (W-31-109-Eng-38) between the U. S. Atomic Energy Commission, Argonne Universities Association and The University of Chicago, the University employs the staff and operates the Laboratory in accordance with policies and programs formulated, approved and reviewed by the Association.

MEMBERS OF ARGONNE UNIVERSITIES ASSOCIATION

The University of Arizona
Carnegie-Mellon University
Case Western Reserve University
The University of Chicago
University of Cincinnati
Illinois Institute of Technology
University of Illinois
Indiana University
Iowa State University
The University of Iowa
Kansas State University
The University of Kansas
Loyola University
Marquette University
Michigan State University
The University of Michigan
University of Minnesota
University of Missouri
Northwestern University
University of Notre Dame
The Ohio State University
Ohio University
The Pennsylvania State University
Purdue University
Saint Louis University
Southern Illinois University
The University of Texas at Austin
Washington University
Wayne State University
The University of Wisconsin

ANL/NDM-10

Cross Sections for (n,p) Reactions on ^{27}Al, $^{46,47,48}Ti$, $^{54,56}Fe$, ^{58}Ni, ^{59}Co and ^{64}Zn from Near Threshold to 10 MeV

by

Donald L. Smith and James W. Meadows

January 1975

Applied Physics Division
Argonne National Laboratory
9700 South Cass Avenue
Argonne, Illinois 60439
U.S.A.

NUCLEAR DATA AND MEASUREMENTS SERIES

The Nuclear Data and Measurements Series presents results of studies in the field of microscopic nuclear data. The primary objective is the dissemination of information in the comprehensive form required for nuclear technology applications. This Series is devoted to: a) Measured microscopic nuclear parameters, b) Experimental techniques and facilities employed in data measurements, c) The analysis, correlation and interpretation of nuclear data, and d) The evaluation of nuclear data. Contributions to this Series are reviewed to assure a high technical excellence and, unless otherwise stated, the contents can be formally referenced. This Series does not surplant formal journal publication but it does provide the more extensive information required for technological applications (e.g. tabulated numerical data) in a timely manner.

TABLE OF CONTENTS

Cross Sections for (n,p) Reactions on ^{27}Al, $^{46,47,48}Ti$, $^{54,56}Fe$, ^{58}Ni, ^{59}Co, and ^{64}Zn from Near Threshold to 10 MeV*

by

Donald L. Smith and James W. Meadows

ABSTRACT

Cross sections for the $^{27}Al(n,p)^{27}Mg$, $^{46,47,48}Ti(n,p)^{46,47,48}Sc$, $^{54,56}Fe(n,p)^{54,56}Mn$, $^{58}Ni(n,p)^{58}Co$, $^{59}Co(n,p)^{59}Fe$ and $^{64}Zn(n,p)^{64}Cu$ reactions have been measured by the activation method for neutron energies from near threshold to $\sim$ 10 MeV. Measurements were made relative to the ^{235}U ($E_n \lesssim 4$ MeV) and ^{238}U ($E_n \gtrsim 4$ MeV) fission cross sections using a fission detector neutron flux monitor. The results are compared with representative data from previously reported investigations. Tables of evaluated cross sections derived from the present work are presented for use in applications.

*This work supported by the U.S. Atomic Energy Commission.

I. INTRODUCTION

Several (n,p) reactions play important roles in nuclear applications. An example is neutron dosimetry. Spectrum unfolding methods are used to deduce neutron dose and spectral information from the activity produced by (n,p) and other reactions in irradiated samples [1,2,3]. The (n,p) process is also important as a mechanism for producing radiation damage in nuclear reactors. These considerations are relevant to both fission reactors and proposed controlled fusion systems (CTR). Thus, accurate knowledge of the cross section excitation functions for (n,p) reactions on various materials which are used as dosimetry monitors or are found in reactor environments is required for current and proposed nuclear-energy programs. Unfortunately, much of the required data is unavailable or insufficiently accurate, and there are discrepancies in the reported cross section sets [4,5]. This need is indicated by the presence of numerous (n,p) reactions on various nuclear data request lists [6,7,8].

Some of the discrepancies can be traced to a lack of standardization in neutron flux determination in the microscopic (n,p) cross section measurements. Another problem is that many of the measurements were performed over limited neutron-energy ranges. In order to increase the neutron-energy ranges, experimenters have often relied upon kinematic effects associated with the use of light-target neutron-source reactions and performed irradiations with samples placed at several neutron emission angles. While this technique is reasonable in principle, it introduces the possibility of making serious systematic errors.

We have undertaken a program of activation cross section measurements for neutron-induced reactions which are important for various nuclear applications. Our objective is to perform systematic measurements over a broad range of energies using a consistent method for measuring neutron flux and taking the necessary precau-

tions to eliminate some possible sources of systematic error. This paper is a report of our work on the $^{27}Al(n,p)^{27}Mg$, $^{46,47,48}Ti(n,p)^{46,47,48}Sc$, $^{54,56}Fe(n,p)^{54,56}Mn$, $^{58}Ni(n,p)^{58}Co$, $^{59}Co(n,p)^{59}Fe$, and $^{64}Zn(n,p)^{64}Cu$ reactions from near threshold to $\sim$ 10 MeV.

II. EXPERIMENTAL PROCEDURES

A. General Measurement Procedure

Samples of high-purity natural metals in the form of 2.54-cm-dia by 0.3-0.6 cm thick disks were used for all measurements. The materials used to fabricate these samples were analyzed by spectrochemical methods to determine the impurities content. No significant impurities were found in any of the samples other than the nickel samples. This is discussed in Section II.F.

During irradiation, each sample was fastened to a low-mass fission detector which served as the neutron flux monitor [9]. This ionization chamber was made from a cylindrical steel can with 0.025-cm-thick walls. The samples were placed outside the chamber; the backing plates with uranium deposits were mounted inside the chamber adjacent to the samples, as shown in Fig. 1. Methane at 1 atm served as the gaseous medium for the ionization chamber. A discriminator was used to reject noise and alpha pulses; pulses above the discrimination level were recorded as fission events in the detector.

The uranium deposits were 2.54 cm in diameter and were fabricated by evaporating UF_4 isotopically enriched in ^{235}U and ^{238}U onto thin, metal backing plates. The isotope contents of these materials were determined by mass spectrographic analysis; the quantity of uranium in each deposit was deduced from measurements of the specific alpha activities [10]. The masses of fissionable-material deposits used in the fission detector were in the range of 0.5-5 milligrams. The deposits enriched in ^{235}U were used for measurements with $E_n \lesssim 4$ MeV; deposits enriched in ^{238}U were used for measurements with $E_n \gtrsim 4$ MeV in order to minimize the corrections for low-energy neutrons.

Irradiations were conducted at the Argonne National Laboratory Fast-Neutron Generator Facility [11]. Neutrons with energies in the

range 0.4-5.5 MeV were produced via the $^{7}Li(p,n)^{7}Be$ reaction (proton energy range 2.15-7.2 MeV). Natural lithium metal was evaporated on tantalum cups to make these targets. Neutrons with energies in the range 5.4-10.2 MeV were produced via the $D(d,n)^{3}He$ reaction (deuteron energy range 2.15-7.0 MeV). A 2-cm-long gas cell containing deuterium gas at 2 atm was used for a target. The sample and fission detector were placed on the beam line 3 to 6 cm from the target for these measurements. There are various differences in the experimental techniques associated with use of these two types of targets. The neutron spectrum from the lithium target becomes complex at higher energies because of the presence of neutrons from the $^{7}Li(p,n)^{7}Be^{*}$ and $^{7}Li(p,n^{3}He)^{4}He$ reactions. The presence of neutrons from the D(d,np)D reaction complicates the neutron spectrum from the deuterium source at higher energies. Methods for coping with these problems are discussed in other reports [12,13,14]. Background measurements were performed during irradiations made using both lithium and deuterium targets to determine the effects of neutrons from the tantalum cups and empty gas-target assembly respectively.

The activities of irradiated samples were measured using standard gamma-ray counting techniques. Most of the counting was done using Ge(Li) detectors; however, all the aluminum and some of low-activity nickel samples were counted with NaI(Tℓ) scintillation detectors. The relative gamma-ray full-energy peak efficiency vs. energy was measured for each detector using a method described by Freeman and Jenkin [15]. The absolute efficiency of each detector was determined at 0.811 and 1.274 MeV by counting ^{58}Co and ^{22}Na standard sources respectively; the absolute activities of these standards were determined by coincidence-counting techniques. Monte-Carlo calculations were made to correct the data for differences in counting efficiencies resulting from absorption and geometric factors. In addition, sum-coincidence and deadtime corrections were determined where required.

Two of the product nuclei (^{46}Sc and ^{58}Co) were produced in isomeric states as well as their ground states. In both cases the upper state decays to the ground state with a half-life that is short compared to the ground state half life. The isomeric activities were permitted to expire before the samples were counted. Therefore, our cross sections are the sums of the partial cross sections for excitation of all accessible states in the product nuclei.

B. Data Processing and Error Analysis

Cross sections for the (n,p) reactions were computed relative to the ^{235}U and ^{238}U fission cross sections after correcting the data for a variety of experimental effects. The requisite fission cross sections were obtained from the Evaluated Neutron Data File, ENDF/B-III [16]. Pertinent values of these fission cross sections are listed in Table I.

Corrections for the neutron source properties were deduced from data obtained from measurements made at our own laboratory [12,13,14] and from a paper by Liskien and Paulsen [17]. The raw data were corrected as required for sample activities and fissions produced by neutrons from the bare target assemblies. Corrections were computed to account for geometric factors and the effects of neutron absorption and multiple scattering. The raw fission counts were corrected for deposit thickness effects, thermal background (for ^{235}U deposits) and low-pulse-height fission events rejected along with the noise and alpha pulses.

The raw sample-count data were corrected for decay half-life and other essential time factors. Factors to account for specific decay properties of the product nuclei, detector efficiency, counting geometry, deadtime losses, gamma-ray absorption, and coincidence summing were applied to the time-corrected data.

The energy resolution for the measurements was governed by target thickness and kinematic broadening. Kinematic broadening was the dominant factor in measurements with the deuterium target.

Generally, the neutron-energy resolutions were 0.04-0.2 MeV for the lithium target measurements and 0.3-0.4 MeV for the deuterium target measurements.

Uncertainties in the measured cross sections can be attributed to statistics as well as a variety of other experimental factors. Table II is representative of the estimated uncertainties, but this table does not necessarily apply to every measured data point reported in this paper. All partial uncertainties were combined in quadrature to determine the overall uncertainties for the measured cross sections. The uncertainties in the fission cross sections and in the decay branching factors for the product nuclei were not included in the assigned error bars. Our measured values could be easily adjusted to accommodate possible future revisions in these parameters.

C. ^{27}Aℓ Measurements

Natural aluminum is entirely ^{27}Aℓ [18]. The Q-value for the ^{27}Aℓ(n,p)^{27}Mg reaction is -1.827 MeV [19,20]. We have used the value of 567.7 ± 0.7 sec for the half life which was measured by Replace [21]. This value is in good agreement with the weighted mean value of several earlier measurements as compiled by Endt and Van der Leun [20]. The daughter ^{27}Mg decays 100% via β^- transitions from the ground state to the first two excited states in ^{27}Aℓ at 0.843 and 1.013 MeV excitation. All disintegrations of ^{27}Mg lead to either a 0.843 or 1.013 MeV gamma ray. We measured the relative yield of these gamma rays and obtained the value of 2.68. The 1.013 MeV state in ^{27}Aℓ decays 97% of the time to the ground state and 3% of the time to the 0.843 MeV state. This implies a value of 28% for the β^- branch to the 1.013-MeV state and 72% for the β^- branch to the 0.843-MeV state. Our value is consistent with the results of recent measurements by Bigoni et al. [22]. We obtained good agreement in the cross section values computed via use of the independent yields of these two gamma rays as well as their sum. Since only about 1% of the ^{27}Mg disintegrations produce

gamma-ray cascades, the corrections for coincidence summing were negligible.

D. ^{46,47,48}Ti Measurements

We measured (n,p) cross sections for ^{46}Ti (7.93% abundance), ^{47}Ti(7.28% abundance) and ^{48}Ti (73.94% abundance) [18]. The Q-values for the ^{46,47,48}Ti(n,p)^{46,47,48}Sc reactions are -1.585, + 0.183 and -3.208 MeV respectively [19].

The decay scheme for ^{46}Sc is quite unambiguous [23]. Nearly 100% of the disintegrations proceed via β^- emission to the 2.010-MeV second-excited state in ^{46}Ti with a half life of 83.8 days. This state de-excites nearly 100% of the time via a gamma-ray cascade through the 0.889-MeV first-excited state in ^{46}Ti. We measured the yields of both gamma rays; cross sections computed from the separate yields were in good agreement with each other. A correction for coincidence summing was made which amounted to $\sim$ 8%.

The decay of ^{47}Sc proceeds 100% of the time via β^- emission to either the ground state or 0.159-MeV first-excited state of ^{47}Ti with a 3.40-day half life [24]. We have used the value of 68.5 ± 2.7% reported by Bak and Riehs for the β^- branch to the 0.159-MeV state in our calculations [25]. The 0.159-MeV state in ^{47}Ti, populated by β^- decay of ^{47}Sc, promptly decays to the ground state by emitting a 0.159-MeV gamma-ray. Consequently, there are 0.685 0.159-MeV gamma-rays per disintegration of ^{47}Sc. The 0.159-MeV gamma-ray activity was measured and used for the cross section calculations. No coincidence-summing corrections were required.

^{48}Sc decays 100% of the time via β^- emission with a half life of 43.8 hours to excited states in ^{48}Ti generating a rather complicated gamma-ray spectrum [26]. Fortunately, there are very nearly 0.98 gamma rays of 1.037 MeV, 1.000 gamma rays of 0.983 MeV and 1.000 gamma rays of 1.312 MeV per disintegration of ^{48}Sc. The yields of each of these gamma-rays were measured. The cross sections computed from these individual transitions were in good agreement. The correction required for coincidence summing was $\sim$ 16% for each case.

E. ^{54,56}Fe Measurements

We have measured (n,p) cross sections for ^{54}Fe (5.82% abundance) and ^{56}Fe (91.66% abundance) [18]. The Q-values for the ^{54,56}Fe(n,p) ^{54,56}Mn reactions are + 0.088 and - 2.917 MeV respectively [19].

The ground state of ^{54}Mn decays with a 312-day half life 100% of the time by electron capture to the 0.835-MeV first-excited state of ^{54}Cr [27]. This state decays via gamma-ray emission to the ground state with a half life of 8.9 ps. No coincidence summing corrections are required.

The ground state of ^{56}Mn decays with a 2.58-hour half life via β^- emission to several excited states in ^{56}Fe [28]. The gamma-ray spectrum for ^{56}Mn is complex, but it happens that there are 0.988 gamma-rays of 0.847-MeV produced for each ^{56}Mn disintegration. We measured the 0.847-MeV gamma-ray yields and computed cross sections for the ^{56}Fe(n,p)^{56}Mn reaction from these data. A correction of $\sim$ 3.3% was required for coincidence summing.

F. ^{58}Ni Measurements

The abundance of ^{58}Ni in natural nickel is 67.88% [18]. The only significant contaminant in the sample disks was 0.106 ± 0.005% cobalt. The ^{59}Co(n,γ)^{60}Co reaction produces background which affected the data for measurements with E_n < 0.8 MeV. Corrections for this background were made using (n,γ) cross sections from an evaluation by Simons McElroy [29] and spectral data from our own measurements. The Q-value for the ^{58}Ni(n,p)^{58}Co reaction is + 0.395 MeV [19]. The ground state of ^{58}Co decays with a 71.3-day half life by a mixture of β^+ emission and electron capture to levels of ^{58}Fe [30]. There are 0.995 gamma rays of 0.811 MeV per ^{58}Co disintegration. We deduced the ^{58}Ni(n,p)^{58}Co reaction cross section from the measured yield of 0.811-MeV gamma rays. A correction of $\sim$ 2.8% was required for coincidence-summing effects.

G. ^{59}Co Measurements

Natural cobalt is entirely ^{59}Co [18]. The Q-value for the ^{59}Co(n,p)^{59}Fe reaction is - 0.783 MeV [19]. The ground state of

^{59}Fe decays entirely by β^- emission to states in ^{59}Co with a half life of 45.1 days [31]. Fortunately, all but 0.3% of the ^{59}Fe disintegrations produce either a 1.099-MeV or 1.292-MeV gamma-rays. We measured the yields of both of these gamma rays and summed the yields after applying appropriate corrections. The (n,p) reaction cross section was therefore determined without concern for the specific branching ratios of these transitions. The coincidence summing correction was $\sim$ 1%.

H. ^{64}Zn Measurements

The isotope ^{64}Zn is 48.89% abundant in natural zinc [18]. The Q-value for the ^{64}Zn(n,p)^{64}Cu reaction is + 0.209 MeV [19]. The ground state of ^{64}Cu decays with a half life of 12.71 hours [32]. Unfortunately, the decay properties of ^{64}Cu are not very conducive to accurate measurement of ^{64}Zn(n,p)^{64}Cu cross sections. The principal decay mode is electron capture to the ground state of ^{64}Ni (40.5% of all disintegrations). Nearly as important is the β^- decay branch to the ground state of ^{64}Zn (39.6% of all disintegrations). There is also a β^+ emission branch to the ground state of ^{64}Ni (19.3% of all disintegrations) and an electron-capture branch of 0.6% to the 1.346-MeV first-excited state in ^{64}Ni. We counted 0.511-MeV gamma rays from annihilation of the emitted β^+ particles and assumed a value of 0.386 annihilation gamma rays per disintegration. The necessity of having to count annihilation radiation limited our ability to make cross section measurements for low neutron energies. Low-level annihilation radiation is present as background in our counting facility and its presence introduced uncertainties in the measurement of the β^+ activity of the zinc samples irradiated at low energies. No sum-coincidence corrections were required for the data.

III. EXPERIMENTAL RESULTS AND DISCUSSION

Results from selected published works are compared with our own data in this section. The data available for comparison are very limited for several of these reactions; for others the available data are extensive and we limited our selection to sets covering

wide neutron-energy ranges. All the data discussed were derived from microscopic rather than integral measurements.

A. $^{27}Al(n,p)^{27}Mg$ Reaction

Our excitation function for this reaction is presented in Fig. 2 and Table III. The structure which we observe is characteristic of (n,p) reactions on light nuclei. Our data is in very good agreement with the work of Hughes and Schwartz in regard to both the structure of the excitation function and normalization [33]. The data of Bass et al. [34] and of Calvi et al. [35] are not in as good agreement. The cross sections of Bass et al. [34] are larger than ours over the entire range of their measurements and the difference increases with neutron energy. These cross sections were measured using neutron scattering from hydrogen as a standard. The cross sections of Calvi et al. [35] were normalized to those of Hughes and Schwartz [33] in the range 4.5-5 MeV. At lower energies, the structure in the excitation function measured by Calvi et al. [35] differs from both the present work and that of Hughes and Schwartz [33].

B. $^{46,47,48}Ti(n,p)^{46,47,48}Sc$ Reactions

Our measured cross sections for the $^{46}Ti(n,p)^{46}Sc$ reaction appear in Fig. 3 and Table IV. There is very little data available to compare with the results of our work. Measurements by Lukic and Carroll provide data for comparison in the region E_n = 5 - 7 MeV [36]. The agreement with our own work is fairly good even though the curve appears to be systematically high relative to our data. The data of Ghorai et al. span the range E_n = 4.1-6.1 MeV and differ considerably from our own results [37]. It is not clear why these data are so different since Ghorai et al. [37] have used the $^{27}Al(n,p)^{27}Mg$ reaction and the evaluated cross sections from Grundl [1] for normalization; the evaluated $^{27}Al(n,p)^{27}Mg$ cross sections from Grundl [1] are in reasonably good agreement with results from the present work.

Our data for the $^{47}Ti(n,p)^{47}Sc$ reaction are presented in Fig. 4 and Table V. Three reported data sets are also plotted on Fig. 4 for comparison [37,38,39]. Of these three sets, only the data of Armitage

[38] is in good agreement with the present work. Armitage made an absolute measurement at one energy and relied upon the $^{58}Ni(n,p)^{58}Co$ cross section data of Barry [40] to normalize the data elsewhere. The data of Ghorai et al. [37] is systematically high relative to our own. This problem was discussed in the preceding paragraph as it applied to the $^{46}Ti(n,p)^{46}Sc$ reaction data as well. The data of Gonzalez et al. [39] differ with our own in regard to both the structure and magnitude except for $E_n \sim 3.5$ MeV. These data were measured relative to the $^{31}P(n,p)^{31}Si$ reaction assuming a standard value of 0.0962 barn for $E_n = 3.56$ MeV. Since we have no data for the $^{31}P(n,p)^{31}Si$ reaction, we cannot comment on this disagreement.

Our data for the $^{48}Ti(n,p)^{48}Sc$ reaction appear in Fig. 5 and Table VI. The only data set which we were able to obtain for comparison with our own is that of Lukic and Carroll [36]. The agreement at $\sim$ 6.5 MeV is good, but elsewhere the two data sets disagree.

C. $^{54,56}Fe(n,p)^{54,56}Mn$ Reactions

These reactions are important for reactor dosimetry and several data sets are available. In general, these data are in reasonably good agreement with our own.

Our results for the $^{54}Fe(n,p)^{54}Mn$ reaction appear in Fig. 6 and Table VII. Data from various reported measurements are also plotted on Fig. 6. The data of Paulsen and Widera [41], Lauber and Malmskog [42], Salsbury and Chalmers [43] and Carroll and Smith [44] are generally in good agreement with our data within the assigned experimental uncertainties. These four sets of measurements were made using the neutron-hydrogen scattering process for neutron-flux determination while our own measurements utilized uranium fission. The observed agreement supports our experimental method which makes use of a fission chamber for neutron-flux monitoring. We have also plotted the data of Van Loef [45] which was normalized relative to an assumed standard value of 0.0962 barn for the $^{31}P(n,p)^{31}Si$ reaction at $E_n = 3.56$ MeV. The agreement of this data set with the rest of the data plotted in Fig. 6 is good at $E_n \sim 3.5$ MeV, but at lower

energies it is poor. A similar difference was indicated for the $^{47}Ti(n,p)^{47}Sc$ reaction in Section III.B (e.g. see Fig. 4).

Our cross sections for the $^{56}Fe(n,p)^{56}Mn$ reaction appear in Fig. 7 and Table VIII. The data of Liskien and Paulsen [46] and Terrel and Holm [47] are in good agreement with our work within the assigned errors. The data of Santry and Butler [48] appear systematically higher than our values although the difference is not great. These authors utilized the $^{32}S(n,p)^{32}P$ reaction as a standard, and they relied on cross section values from Allen et al. [49] for this reaction.

D. $^{58}Ni(n,p)^{58}Co$ Reaction

This reaction is one of the most widely used (n,p) reactions in reactor dosimetry applications. Consequently, there is a great deal of data available [4,5]. There have been several recent evaluations reported (e.g. Refs. 2,41,50 and 51). These evaluations are not in very good agreement as can be surmised from Fig. 3 of Ref. 41. The presence of pronounced structure in the evaluation by Bresesti et al. [50] in the region of E_n = 3-4 MeV is the result of assignment of considerable weight to the data of Konijn and Lauber [52]. This structure appeared to us to be anamolous for an (n,p) reaction in this mass region. Therefore, we made two sets of cross section measurements for the $^{58}Ni(n,p)^{58}Co$ reaction. The first set of measurements yielded an excitation function from threshold to $\sim$ 10 MeV with neutron-energy resolution equivalent to that for other data sets reported herein. The results of this set of measurements appear in Fig. 8 and Table IX, Part A. The second set of measurements was made with neutron-energy resolution of $\sim$ 0.04 MeV over the range E_n = 2.85-4.02 MeV. This resolution is superior to that reported by Konijn and Lauber [52]. The results of this set of fine-resolution measurements are presented in Fig. 9 and Table IX, Part B. We find no evidence for the pronounced resonance structure observed by Konijn and Lauber [52]. The data reported by Konijn and Lauber [52] was obtained by means of proton detection using a silicon

solid-state detector. It may be that the observed structure was an anomaly associated with this measurement technique since none of the reported data from activation measurements show similar structure.

There are several reported data sets which are in very good agreement with our excitation function. Our excitation function is compared with the data of Barry [40], Paulsen and Widera [41], Meadows and Whalen [53] and Nakai et al. [54] in Fig. 8. The data of Barry [40] appears systematically higher than our data; however, this set is in agreement with our work within the assigned uncertainties. In view of the agreement of these four data sets with our own data, we chose not to plot a number of other data sets which differ from our data; to do so would merely complicate Fig. 8 and not add any useful information.

E. $^{59}Co(n,p)^{59}Fe$ Reaction

The results of our cross section measurements for this reaction appear in Fig. 10 and Table X. There are no other data available for comparison.

F. $^{64}Zn(n,p)^{64}Cu$ Reaction

Our data for this reaction are presented in Fig. 11 and Table XI. Three other data sets are plotted on Fig. 11 for comparison [54,55,56]. None of these data are in very good agreement with our work. The excitation function of Rapaport and Van Loef [55] differs from ours with regard to shape although the measured cross section for $E_n \sim 2.5$ MeV is in agreement. The excitation function of Nakai et al. [54] also differs in shape although their cross section values for E_n = 2-3 MeV are in fairly good agreement with our work. The cross section values of Santry and Butler [56] are considerably larger than ours over the entire range of their measurements. For $E_n \sim 10$ MeV the discrepancy is nearly a factor of 2.

We can offer no particular explanation for these differences. It should be restated that in addition to the usual neutron-fluence-measurement problems, one must cope with the rather unfavorable

decay properties of ^{64}Cu, as discussed in Section II.H, in measuring cross sections for this reaction.

IV. EVALUATED DATA

Measured cross section values, such as those in Tables III-XI, representing the results of the present work, do not provide information in a form which is particularly useful for applications. These cross sections exhibit fluctuations characteristic of experimental data; repeated measurements improve data reliability but also generate redundancy. What is required are evaluated cross sections which exhibit all essential features of the data exclusive of insignificant experimental fluctuations and redundancy. The $^{235,238}U$ fission cross sections given in Table I are examples.

We have made an evaluation of our (n,p) data by plotting these data on semilog paper, drawing smooth curves through the data points, and selecting a sufficient number of points on these curves to permit reproduction of the excitation functions. The evaluated (n,p) cross sections for ^{27}Al, $^{46,47,48}Ti$, $^{54,56}Fe$, ^{58}Ni, ^{59}Co and ^{64}Zn appear in Tables XII-XX respectively. Cross sections for energies other than those appearing in the tables can be estimated from the formulas

$$\ln \sigma = a + b \ln E \qquad (1)$$

$$a = (E_2 \ln \sigma_1 - E_1 \ln \sigma_2)/(E_2 - E_1) \qquad (2)$$

$$b = (\ln \sigma_2 - \ln \sigma_1)/(E_2 - E_1) \qquad (3)$$

where (E_1, σ_1) and (E_2, σ_2) are adjacent entries in the table and $E_1 < E < E_2$. These formulas can also be used to estimate the corresponding fission cross sections using values from Table I. Figure 12 exhibits plots of the evaluated (n,p) cross sections as well as the ^{235}U and ^{238}U fission cross sections. Since these are isotopic cross sections, the relative importance of the various (n,p) reactions can be deduced by taking the relative isotopic abundances in natural metals into consideration.

REFERENCES

1. J. A. Grundl, Nucl. Sci. Eng., 30, 39 (1967).
2. R. L. Simons and W. N. McElroy, "Evaluated Reference Cross Section Library," BNWL-1312, Pacific Northwest Laboratories, Battelle Memorial Institute (1970).
3. W. Köhler, Rev. Atomic Energy, 9, 441 (1971).
4. "Experimental Data File (CSISRS)," National Neutron Cross Section Center, Brookhaven National Laboratory.
5. H. Liskien and A. Paulsen, "Compilation of Cross Sections for Some Neutron-Induced Threshold Reactions," EUR 1.19.e, Vols. 1 and 2, Central Bureau for Nuclear Measurements, Geel, Belgium (1968).
6. "Compilation of Requests for Nuclear Data," USNDC-6 (LA-5253-MS), Los Alamos Scientific Laboratory (1974).
7. "WRENDA-74, World Request List for Nuclear Data Measurements-Fission Reactor Programmes," INDC(SEC)-38/U, International Atomic Energy Agency (1974).
8. "Request Lists of Nuclear Data for Controlled Fusion Research as Submitted to the International Atomic Energy Agency by Member States," INDC(NDS)-57/U+F, ed. J. R. Lemley, International Atomic Energy Agency (1973).
9. R. W. Lamphere, "Fission Detectors," in Fast Neutron Physics I, eds. J. B. Marion and J. L. Fowler, Interscience, New York, p.721 (1960).
10. J. W. Meadows, Nucl. Sci. Eng., 49, 310 (1972).
11. S. A. Cox and P. R. Hauley, IEE Trans. Nucl. Sci., 18, 108 (1971).
12. J. W. Meadows and D. L. Smith," Neutrons from Proton Bombardment of Lithium," ANL-7938, Argonne National Laboratory (1972).
13. Donald L. Smith and James W. Meadows, "Measurement of $^{58}Ni(n,p)^{58}Co$ Reaction Cross Sections for E_n = 0.44-5.87 MeV Using Activation Methods," ANL-7989, Argonne National Laboratory (1973).
14. D. L. Smith and J. W. Meadows, "Method of Neutron Activation Cross Section Measurement for E_n = 5.5-10 MeV Using the $D(d,n)^3He$ Reaction as a Neutron Source," ANL/NDM-9, Argonne National Laboratory (1974).
15. J. M. Freeman and J. G. Jenkin, Nucl. Instr. Meth., 43, 269 (1966).
16. "Evaluated Neutron Data File, ENDF/B-III," National Neutron Cross Section Center, Brookhaven National Laboratory.
17. H. Liskien and A. Paulsen, Nucl. Data, 11-7, 569 (1973).

18. C. A. Rohrman, "Chart of the Nuclides," compiled at Battelle-North-West Laboratories, Richland, Washington, for the U.S. Atomic Energy Commission (1969).
19. F. Ajzenberg-Selove and C. L. Busch, "Nuclear Wallet Cards," prepared for the American Physical Society (1971); see also A. H. Wapstra and N. B. Gove, Nucl. Data Tables 9, 267 (1971).
20. P. M. Endt and C. Van der Leun, Nucl. Phys. A105, 1 (1967).
21. J. L. Replace, Radiochim. Acta 14, 46 (1970).
22. R. A. Bigoni, S. D. Bloom and K. G. Tirsell, Nucl. Phys. A134, 620 (1969).
23. R. L. Auble, Nuclear Data B4, 269 (1970).
24. M. B. Lewis, Nuclear Data B4, 313 (1970).
25. Zong-Tschun Bak and P. Riehs, Int. J. Appl. Radiat. Isotop. 19, 593 (1968).
26. J. Rapaport, Nuclear Data B4, 351 (1970).
27. H. Verheul, Nuclear Data B3-5, 6-163 (1970).
28. M. N. Rao, Nuclear Data B3-3, 4-43 (1970).
29. R. L. Simons and W. N. McElroy, "Evaluated Reference Cross Section Library," BNWL-1312 (1970).
30. S. Raman, Nucl. Data B3-3, 4-145 (1970).
31. J. Vervier, Nucl. Data B2-5, 1 (1968).
32. R. L. Auble, Nucl. Data Sheets 12-3, 305 (1974).
33. D. J. Hughes and R. B. Schwartz, BNL-325 (1958).
34. R. Bass, P. Haug, K. Kruger and B. Staginnus, EANDC (E) 66, 64 (1966).
35. G. Calvi, R. Potenza, R. Ricamo and D. Vinciguerra, Nucl. Phys. 39, 621 (1962).
36. Y. Lukic and E. E. Carroll, Nucl. Sci. Eng. 43, 233 (1971).
37. S. K. Ghorai, J. R. Cooper, J. D. Moore and W. L. Alford, Jour. Nucl. Energy 25, 319 (1971).
38. F. G. Armitage; Transmitted to the National Neutron Cross Section Center, Brookhaven National Laboratory, by J. Symonds (1967). Data available from the CSISRS file.
39. L. Gonzalez, A. Trier and J. J. Van Loef, Phys. Rev. 126, 271 (1962).
40. J. F. Barry, Jour. Nucl. Energy A/B 16, 467 (1962).
41. A. Paulsen and R. Widera, "$^{58}Ni(n,p)^{58}Co$ and $^{54}Fe(n,p)^{54}Mn$ Cross Section Measurements for Use as Threshold Detectors," in Chemical Nuclear Data: Measurements and Applications, M. L. Wurrell, ed., Institution of Civil Engineers, London (1971).

42. A. Lauber and S. Malmskog, Nucl. Phys. 73, 234 (1965).
43. S. R. Salsbury and R. A. Chalmers, Phys. Rev. 140, B305 (1965).
44. E. E. Carroll and G. G. Smith, Nucl. Sci. Eng. 22, 411 (1965).
45. J. J. Van Loef, Nucl. Phys. 24, 340 (1961).
46. H. Liskien and A. Paulsen, Nukleonik 8, 315 (1966.
47. J. Terrel and D. M. Holm, Phys. Rev. 109, 2031 (1958).
48. D. C. Santry and J. P. Butler, Can. J. Phys. 42, 1030 (1964).
49. L. Allen, Jr., W. A. Biggers, R. J. Prestwood and R. K. Smith, Phys. Rev. 107, 1363 (1957).
50. A. M. Bresesti, M. Bresesti, A. Rota, R. A. Rydin and L. Lesca, Nucl. Sci. Eng. 40, 331 (1970).
51. A. Fabray and J. C. Schepers, "Some Nuclear Data and Considerations Related to Reactor Dosimetry With Threshold Detectors," Report to the EURATOM Dosimetry Working Group, CEN-Mol (1970).
52. J. Konijn and A. Lauber, Nucl. Phys. 48, 191 (1963).
53. J. W. Meadows and J. F. Whalen, Phys. Rev. 130, 2022 (1963).
54. K. Nakai, H. Gotch and H. Amano, Jour. Phys. Soc. Japan 17, 1215 (1962).
55. J. Rapaport and J. J. Van Loef, Phys. Rev. 114, 565 (1959).
56. D. C. Santry and J. P. Butler, Bull. Am. Phys. Soc. 12, 481 (1967).

TABLE I

^{235}U and ^{238}U Fission Cross Sections

Used in the Present Work[a]

A. $^{235}U(n,f)$ Cross Sections

E_n (MeV)	σ_F (barn)	E_n (MeV)	σ_F (barn)	E_n (MeV)	σ_F (barn)
0.0[b]	580.0	0.8	1.133	6.1	1.098
1.0×10^{-6}	65.0	0.85	1.15	6.3	1.164
0.001	8.05	0.95	1.218	6.8	1.413
0.003	4.99	1.0	1.235	7.2	1.552
0.01	3.21	1.5	1.247	7.6	1.634
0.0175	2.7	2.0	1.315	8.5	1.751
0.03	2.27	2.3	1.309	9.5	1.753
0.055	1.91	2.6	1.281	10.5	1.7
0.1	1.635	3.2	1.177		
0.16	1.478	3.6	1.146		
0.24	1.32	4.2	1.089		
0.35	1.225	4.8	1.056		
0.4	1.218	5.4	1.046		
0.54	1.16	5.8	1.068		

B. $^{238}U(n,f)$ Cross Sections

E_n (MeV)	σ_F (barn)	E_n (MeV)	σ_F (barn)	E_n (MeV)	σ_F (barn)
0.0[b]	0.0	1.514	0.3458	4.47	0.5339
0.5	2.34×10^{-4}	1.617	0.4169	5.08	0.5324
0.61	1.24×10^{-3}	1.72	0.4472	5.33	0.5403
0.75	1.98×10^{-3}	1.821	0.5122	6.0	0.618
0.85	5.87×10^{-3}	1.914	0.5397	7.0	0.936
0.898	0.0123	2.0	0.5371	7.5	0.978
1.005	0.0163	2.51	0.5573	8.5	1.0
1.108	0.0273	3.08	0.525	10.0	0.974
1.205	0.0374	3.28	0.5242	12.0	0.995
1.306	0.0651	3.58	0.5352		
1.401	0.1939	4.08	0.5336		

a. Cross section values selected from Ref. 16 files to construct a representation of the fission cross section excitation function—exclusive of resonance effects.

b. Data processing code requires a "zero-energy" cross section.

TABLE II

Typical Values for the Principal Sources of Uncertainty in the Measured Cross Sections

Source of Uncertainty	Uncertainty
1. Counting statistics	1 - 10%
2. Integration of gamma-ray full-energy peak	3%
3. Gamma-ray detector efficiency	3%
4. Decay half life	< 1%
5. Fission deposit and sample dimensions	1.4%
6. Neutron-group intensities	1-4%
7. Scattering corrections	1%
8. Weight of Uranium deposits	1%
9. Miscellaneous errors	1%

TABLE III

Measured Cross Sections for the $^{27}Al(n,p)^{27}Mg$ Reaction

E_n (MeV)	Resolution (MeV)	σ_{np} (barn)	$\pm \Delta\sigma_{np}$ (barn)
.2805E 01	.5818E-01	.3508E-03	.6367E-04
.2856E 01	.5831E-01	.4524E-03	.4111E-04
.2905E 01	.5843E-01	.7220E-03	.6360E-04
.2956E 01	.5857E-01	.7713E-03	.3671E-04
.3006E 01	.5870E-01	.1046E-02	.6533E-04
.3057E 01	.5885E-01	.1009E-02	.6165E-04
.3107E 01	.5899E-01	.1977E-02	.1074E-03
.3157E 01	.5915E-01	.2050E-02	.1048E-03
.3206E 01	.5930E-01	.2058E-02	.1797E-03
.3257E 01	.5946E-01	.2738E-02	.1327E-03
.3306E 01	.5962E-01	.1948E-02	.9944E-04
.3360E 01	.5980E-01	.2225E-02	.1205E-03
.3409E 01	.5997E-01	.4990E-02	.2952E-03
.3459E 01	.6014E-01	.7188E-02	.3746E-03
.3508E 01	.6032E-01	.7887E-02	.4589E-03
.3559E 01	.6051E-01	.5156E-02	.2389E-03
.3610E 01	.6070E-01	.6871E-02	.3235E-03
.3659E 01	.6088E-01	.7064E-02	.3245E-03
.3710E 01	.6108E-01	.6166E-02	.2909E-03
.3758E 01	.6127E-01	.9301E-02	.4279E-03
.3809E 01	.6148E-01	.6004E-02	.2770E-03
.3860E 01	.6168E-01	.4301E-02	.2022E-03
.3910E 01	.6188E-01	.5612E-02	.2728E-03
.3962E 01	.6210E-01	.7247E-02	.3431E-03
.4012E 01	.6231E-01	.6972E-02	.3217E-03
.4062E 01	.6253E-01	.6762E-02	.3195E-03
.4110E 01	.6273E-01	.5261E-02	.2462E-03
.4162E 01	.6296E-01	.4986E-02	.2426E-03
.4212E 01	.6318E-01	.7815E-02	.3581E-03
.4263E 01	.6341E-01	.1048E-01	.4848E-03
.4312E 01	.6363E-01	.1188E-01	.5413E-03
.4363E 01	.6387E-01	.1084E-01	.4975E-03
.4412E 01	.6409E-01	.1067E-01	.4916E-03
.4463E 01	.6433E-01	.1202E-01	.5531E-03
.4512E 01	.6456E-01	.1524E-01	.8978E-03
.4564E 01	.6481E-01	.1848E-01	.8434E-03
.4613E 01	.6505E-01	.2086E-01	.9389E-03
.4664E 01	.6529E-01	.1653E-01	.7436E-03
.4713E 01	.6554E-01	.1906E-01	.9214E-03
.4761E 01	.6577E-01	.1598E-01	.8249E-03
.4814E 01	.6603E-01	.1288E-01	.5898E-03
.4865E 01	.6628E-01	.1578E-01	.7149E-03
.4913E 01	.6652E-01	.2075E-01	.9381E-03
.4964E 01	.6678E-01	.2527E-01	.1153E-02

TABLE III (Cont'd)

E_n (MeV)	Resolution (MeV)	σ_{np} (barn)	$\pm \Delta\sigma_{np}$ (barn)
.5014E 01	.6704E-01	.2905E-01	.1303E-02
.5063E 01	.6730E-01	.2656E-01	.1195E-02
.5113E 01	.6755E-01	.2596E-01	.1177E-02
.5165E 01	.6782E-01	.2989E-01	.1348E-02
.5215E 01	.6808E-01	.3025E-01	.1368E-02
.5263E 01	.6834E-01	.2830E-01	.1301E-02
.5314E 01	.6861E-01	.2423E-01	.1146E-02
.5365E 01	.6888E-01	.3075E-01	.1386E-02
.5415E 01	.6915E-01	.3143E-01	.1487E-02
.5466E 01	.6942E-01	.3857E-01	.1742E-02
.5515E 01	.6969E-01	.4407E-01	.1988E-02
.5563E 01	.6996E-01	.4295E-01	.1945E-02
.5614E 01	.7024E-01	.4664E-01	.2124E-02
.5666E 01	.7052E-01	.4779E-01	.2143E-02
.5714E 01	.7078E-01	.6915E-01	.3092E-02
.5765E 01	.7107E-01	.5922E-01	.2656E-02
.5818E 01	.6145E-01	.4512E-01	.2099E-02
.5871E 01	.6179E-01	.4437E-01	.2242E-02
.5920E 01	.6212E-01	.4691E-01	.2183E-02
.5920E 01	.6212E-01	.4571E-01	.2123E-02
.5437E 01	.3340E 00	.3537E-01	.1804E-02
.5707E 01	.3300E 00	.5779E-01	.3063E-02
.5970E 01	.3280E 00	.3910E-01	.2111E-02
.6497E 01	.3320E 00	.4790E-01	.2491E-02
.6756E 01	.3360E 00	.4759E-01	.2428E-02
.7007E 01	.3420E 00	.5643E-01	.2878E-02
.7263E 01	.3480E 00	.6120E-01	.3121E-02
.7515E 01	.3540E 00	.6255E-01	.2329E-02
.7764E 01	.3620E 00	.6923E-01	.3530E-02
.8011E 01	.3700E 00	.7054E-01	.3598E-02
.8257E 01	.3780E 00	.7721E-01	.4015E-02
.8505E 01	.3880E 00	.7657E-01	.3905E-02
.8751E 01	.3940E 00	.8416E-01	.4798E-02
.8995E 01	.4040E 00	.7869E-01	.4485E-02
.9237E 01	.4140E 00	.8368E-01	.4518E-02
.9479E 01	.4240E 00	.8188E-01	.4668E-02
.9710E 01	.4340E 00	.8582E-01	.4891E-02
.9960E 01	.4440E 00	.8968E-01	.5111E-02

TABLE IV

Measured Cross Sections for the $^{46}Ti(n,p)^{46}Sc$ Reaction

E_n (MeV)	Resolution (MeV)	σ_{np} (barn)	$\pm \Delta\sigma_{np}$ (barn)
.3668E 01	.1640E 00	.1310E-01	.2710E-02
.3769E 01	.1640E 00	.1560E-01	.1220E-02
.3983E 01	.1540E 00	.2000E-01	.1200E-02
.4196E 01	.1560E 00	.3520E-01	.3100E-02
.4336E 01	.1560E 00	.3570E-01	.2400E-02
.4398E 01	.1560E 00	.3720E-01	.2400E-02
.4537E 01	.1580E 00	.5690E-01	.3500E-02
.4600E 01	.1560E 00	.4500E-01	.3500E-02
.4721E 01	.1720E 00	.5490E-01	.3090E-02
.4735E 01	.1580E 00	.6380E-01	.3500E-02
.4799E 01	.1580E 00	.5600E-01	.3600E-02
.4937E 01	.1600E 00	.7250E-01	.5000E-02
.4999E 01	.1600E 00	.7280E-01	.4500E-02
.5138E 01	.1600E 00	.7820E-01	.5900E-02
.5198E 01	.1620E 00	.7390E-01	.4500E-02
.5234E 01	.1928E 00	.7400E-01	.1220E-02
.5238E 01	.1620E 00	.8500E-01	.5200E-02
.5438E 01	.1620E 00	.9190E-01	.5600E-02
.5639E 01	.1640E 00	.9750E-01	.6000E-02
.5859E 01	.1660E 00	.9780E-01	.1140E-01
.5938E 01	.1660E 00	.1166E 00	.1240E-01
.5407E 01	.3320E 00	.8800E-01	.6424E-02
.5957E 01	.3260E 00	.1234E 00	.9749E-02
.6996E 01	.3380E 00	.1733E 00	.1733E-01
.7499E 01	.3500E 00	.1842E 00	.1842E-01
.7998E 01	.3640E 00	.2113E 00	.1817E-01
.8491E 01	.3820E 00	.2269E 00	.2337E-01
.8983E 01	.4000E 00	.2172E 00	.2628E-01
.9467E 01	.4180E 00	.2350E 00	.1692E-01
.9950E 01	.4380E 00	.2330E 00	.2703E-01

TABLE V

Measured Cross Sections for the
$^{47}Ti(n,p)^{47}Sc$ Reaction

E_n (MeV)	Resolution (MeV)	σ_{np} (barn)	$\pm \Delta\sigma_{np}$ (barn)
.9140E 00	.1840E 00	.2480E-04	.7790E-05
.1127E 01	.1740E 00	.1220E-02	.1220E-03
.1220E 01	.1040E 00	.2820E-02	.2690E-03
.1305E 01	.1000E 00	.3770E-02	.4600E-03
.1425E 01	.1040E 00	.3050E-02	.3240E-03
.1437E 01	.6000E-01	.3270E-02	.4610E-03
.1542E 01	.6000E-01	.3870E-02	.5920E-03
.1619E 01	.1040E 00	.4820E-02	.4550E-03
.1640E 01	.6200E-01	.5790E-02	.6482E-03
.1822E 01	.1040E 00	.9820E-02	.9360E-03
.1825E 01	.1180E 00	.1120E-01	.1040E-02
.1957E 01	.6600E-01	.1090E-01	.1070E-02
.1978E 01	.1600E 00	.1350E-01	.1080E-02
.2006E 01	.1060E 00	.1540E-01	.1440E-02
.2039E 01	.6600E-01	.1730E-01	.1610E-02
.2142E 01	.6800E-01	.1950E-01	.1620E-02
.2209E 01	.1080E 00	.1820E-01	.1710E-02
.2246E 01	.6800E-01	.2200E-01	.1910E-02
.2351E 01	.6800E-01	.3210E-01	.2630E-02
.2424E 01	.1500E 00	.3370E-01	.2930E-02
.2447E 01	.7000E-01	.3070E-01	.2490E-02
.2654E 01	.7200E-01	.3020E-01	.2570E-02
.2754E 01	.7400E-01	.3060E-01	.2480E-02
.2854E 01	.7600E-01	.3450E-01	.2790E-02
.2968E 01	.7600E-01	.3930E-01	.3180E-02
.3058E 01	.7600E-01	.3900E-01	.3160E-02
.3163E 01	.7800E-01	.4730E-01	.3880E-02
.3260E 01	.8000E-01	.4980E-01	.4080E-02
.3428E 01	.1480E 00	.5110E-01	.4190E-02
.3663E 01	.8400E-01	.5840E-01	.4790E-02
.3666E 01	.1640E 00	.5790E-01	.5410E-02
.3763E 01	.8600E-01	.6210E-01	.5090E-02
.3767E 01	.1640E 00	.6270E-01	.5850E-02
.3861E 01	.8800E-01	.6760E-01	.5540E-02
.3958E 01	.8800E-01	.6380E-01	.5230E-02
.4014E 01	.1100E 00	.5930E-01	.4740E-02
.4063E 01	.9000E-01	.6860E-01	.5590E-02
.4116E 01	.1120E 00	.6380E-01	.5100E-02
.4161E 01	.1220E 00	.6650E-01	.5320E-02
.4170E 01	.9200E-01	.7170E-01	.5880E-02
.4211E 01	.1220E 00	.6520E-01	.5220E-02
.4216E 01	.1120E 00	.6540E-01	.5300E-02
.4272E 01	.9200E-01	.7290E-01	.5980E-02
.4335E 01	.1560E 00	.7060E-01	.5680E-02

TABLE V (Cont'd)

E_n (MeV)	Resolution (MeV)	σ_{np} (barn)	$\pm \Delta\sigma_{np}$ (barn)
.4372E 01	.9600E-01	.7170E-01	.5880E-02
.4444E 01	.1480E 00	.7180E-01	.5890E-02
.4447E 01	.9800E-01	.7110E-01	.5740E-02
.4536E 01	.1560E 00	.7190E-01	.5740E-02
.4581E 01	.1000E 00	.8080E-01	.6480E-02
.4614E 01	.1260E 00	.7010E-01	.5610E-02
.4720E 01	.1720E 00	.7570E-01	.7060E-02
.4734E 01	.1580E 00	.8040E-01	.6430E-02
.4799E 01	.1560E 00	.7280E-01	.5820E-02
.4936E 01	.1600E 00	.7800E-01	.6240E-02
.4999E 01	.1560E 00	.7760E-01	.6210E-02
.5198E 01	.1600E 00	.7460E-01	.5970E-02
.5203E 01	.1560E 00	.7860E-01	.6290E-02
.5233E 01	.1720E 00	.8210E-01	.7660E-02
.5238E 01	.1600E 00	.7650E-01	.6120E-02
.5438E 01	.1640E 00	.8170E-01	.6540E-02
.5448E 01	.1520E 00	.8410E-01	.7230E-02
.5639E 01	.1640E 00	.8940E-01	.7150E-02
.5779E 01	.1640E 00	.9470E-01	.7760E-02
.5839E 01	.1660E 00	.9970E-01	.7980E-02
.5937E 01	.1660E 00	.9630E-01	.7700E-02
.5954E 01	.3260E 00	.9100E-01	.4641E-02
.6995E 01	.3360E 00	.9950E-01	.5075E-02
.7499E 01	.3500E 00	.1083E 00	.5523E-02
.7998E 01	.3640E 00	.1191E 00	.6074E-02
.8491E 01	.3820E 00	.1238E 00	.6314E-02
.8983E 01	.4000E 00	.1309E 00	.6807E-02
.9467E 01	.4180E 00	.1298E 00	.6750E-02
.9950E 01	.4380E 00	.1441E 00	.7781E-02

TABLE VI

Measured Cross Sections for the
$^{48}Ti(n,p)^{48}Sc$ Reaction

E_n (MeV)	Resolution (MeV)	σ_{np} (barn)	$\pm \Delta\sigma_{np}$ (barn)
.4724E 01	.1720E 00	.2800E-04	.3290E-05
.4738E 01	.1580E 00	.3140E-04	.6000E-06
.4938E 01	.1600E 00	.8180E-04	.8000E-06
.5142E 01	.1600E 00	.9510E-04	.1700E-05
.5237E 01	.1760E 00	.2390E-03	.2510E-04
.5241E 01	.1620E 00	.2780E-03	.1800E-04
.5440E 01	.1620E 00	.4140E-03	.2000E-04
.5641E 01	.1640E 00	.5270E-03	.5200E-04
.5841E 01	.1660E 00	.1560E-02	.1940E-03
.5938E 01	.1660E 00	.1255E-02	.7200E-04
.5964E 01	.3260E 00	.1880E-02	.1034E-03
.6488E 01	.3280E 00	.3460E-02	.1834E-03
.6999E 01	.3380E 00	.6820E-02	.3546E-03
.7501E 01	.3500E 00	.9780E-02	.4988E-03
.8000E 01	.3640E 00	.1353E-01	.6900E-03
.8493E 01	.3820E 00	.1587E-01	.8094E-03
.8985E 01	.4000E 00	.1933E-01	.1005E-02
.9469E 01	.4180E 00	.2408E-01	.1276E-02
.9952E 01	.4380E 00	.2666E-01	.1520E-02

TABLE VII

Measured Cross Sections for the $^{54}Fe(n,p)^{54}Mn$ Reaction

E_n (MeV)	Resolution (MeV)	σ_{np} (barn)	$\pm \Delta\sigma_{np}$ (barn)
.1979E 01	.1600E 00	.1270E-01	.1300E-02
.2181E 01	.1580E 00	.2620E-01	.2200E-02
.2589E 01	.1560E 00	.7210E-01	.4000E-02
.2727E 01	.3720E 00	.1190E 00	.6800E-02
.2782E 01	.1600E 00	.9960E-01	.5200E-02
.2792E 01	.1560E 00	.1000E 00	.5400E-02
.2985E 01	.1560E 00	.1320E 00	.7000E-02
.3187E 01	.1600E 00	.1450E 00	.7600E-02
.3385E 01	.1600E 00	.1970E 00	.1100E-01
.3587E 01	.1620E 00	.2650E 00	.1400E-01
.3716E 01	.4360E 00	.2480E 00	.1400E-01
.3788E 01	.1620E 00	.2610E 00	.1400E-01
.3990E 01	.1620E 00	.2490E 00	.1300E-01
.4183E 01	.1640E 00	.3100E 00	.1800E-01
.4385E 01	.1660E 00	.3060E 00	.1600E-01
.4587E 01	.1660E 00	.3310E 00	.1700E-01
.4587E 01	.1660E 00	.3610E 00	.2000E-01
.4795E 01	.1600E 00	.3670E 00	.2100E-01
.4796E 01	.1680E 00	.3640E 00	.1900E-01
.4895E 01	.1620E 00	.3830E 00	.2500E-01
.4996E 01	.1700E 00	.4290E 00	.2400E-01
.4996E 01	.1700E 00	.4010E 00	.2100E-01
.5037E 01	.1620E 00	.3890E 00	.2700E-01
.5137E 01	.1640E 00	.4480E 00	.3600E-01
.5199E 01	.1720E 00	.3890E 00	.2100E-01
.5238E 01	.1640E 00	.4360E 00	.2300E-01
.5255E 01	.1300E 00	.4580E 00	.3600E-01
.5355E 01	.1300E 00	.4150E 00	.3000E-01
.5438E 01	.1660E 00	.4740E 00	.2500E-01
.5407E 01	.3360E 00	.4412E 00	.2294E-01
.5954E 01	.3280E 00	.4592E 00	.2342E-01
.6481E 01	.3320E 00	.4616E 00	.2400E-01
.6996E 01	.3420E 00	.4597E 00	.2436E-01
.7500E 01	.3540E 00	.4652E 00	.2466E-01
.7997E 01	.3700E 00	.4377E 00	.2276E-01
.8491E 01	.3860E 00	.4625E 00	.2590E-01
.8982E 01	.4040E 00	.4909E 00	.2602E-01
.9466E 01	.4240E 00	.4494E 00	.2786E-01
.9948E 01	.4440E 00	.4493E 00	.2561E-01

TABLE VIII

Measured Cross Sections for the $^{56}Fe(n,p)^{56}Mn$ Reaction

E_n (MeV)	Resolution (MeV)	σ_{np} (barn)	$\pm \Delta\sigma_{np}$ (barn)
.3979E 01	.1240E 00	.5160E-05	.3300E-05
.4078E 01	.1240E-01	.1830E-04	.3000E-05
.4178E 01	.1260E 00	.1400E-04	.3800E-05
.4268E 01	.1280E 00	.3710E-04	.3680E-05
.4367E 01	.1280E 00	.7830E-04	.5480E-05
.4479E 01	.1300E 00	.1160E-03	.8300E-05
.4594E 01	.1320E 00	.2050E-03	.1300E-04
.4680E 01	.1340E 00	.3420E-03	.2000E-04
.4781E 01	.1340E 00	.5890E-03	.3200E-04
.4798E 01	.1620E 00	.6820E-03	.3800E-04
.4882E 01	.1360E 00	.7740E-03	.4200E-04
.4896E 01	.1640E 00	.6650E-03	.3600E-04
.4981E 01	.1380E 00	.8040E-03	.5100E-04
.5039E 01	.1640E 00	.1036E-02	.5700E-04
.5140E 01	.1660E 00	.1457E-02	.8000E-04
.5256E 01	.1320E 00	.2060E-02	.1100E-03
.5356E 01	.1320E 00	.2770E-02	.1400E-03
.5456E 01	.1340E 00	.4110E-02	.2100E-03
.5554E 01	.1340E 00	.6020E-02	.3100E-03
.5656E 01	.1360E 00	.7870E-02	.4000E-03
.5756E 01	.1380E 00	.6710E-02	.3500E-03
.5857E 01	.1380E 00	.1290E-01	.6600E-03
.5939E 01	.1720E 00	.1170E-01	.6000E-03
.6486E 01	.3300E 00	.1950E-01	.9750E-03
.7019E 01	.3420E 00	.2690E-01	.1345E-02
.8494E 01	.3860E 00	.4760E-01	.2380E-02
.8983E 01	.4040E 00	.5450E-01	.2800E-02
.9461E 01	.4240E 00	.5750E-01	.3084E-02
.9945E 01	.4440E 00	.6220E-01	.3545E-02

TABLE IX

Measured Cross Sections for the $^{58}Ni(n,p)^{58}Co$ Reaction

A. Excitation function from threshold to ∿ 10 MeV:

E_n (MeV)	Resolution (MeV)	σ_{np} (barn)	$\pm \Delta\sigma_{np}$ (barn)
.4410E 00	.2260E 00	.3230E-05	.5600E-06
.6340E 00	.1260E 00	.2407E-05	.1650E-05
.7240E 00	.1260E 00	.8836E-04	.2500E-05
.8380E 00	.1260E 00	.3039E-03	.4500E-04
.8720E 00	.1820E 00	.3059E-03	.3400E-04
.9300E 00	.1260E 00	.5797E-03	.5000E-04
.1038E 01	.1280E 00	.1083E-02	.7400E-04
.1099E 01	.1760E 00	.2347E-02	.1200E-03
.1138E 01	.1280E 00	.3561E-02	.1700E-03
.1276E 01	.1000E 00	.5546E-02	.7500E-03
.1407E 01	.6000E-01	.1153E-01	.4500E-02
.1503E 01	.6400E-01	.1314E-01	.1100E-02
.1607E 01	.6200E-01	.1575E-01	.1500E-02
.1705E 01	.6400E-01	.2387E-01	.1600E-02
.1803E 01	.6400E-01	.2638E-01	.1360E-02
.1904E 01	.6400E-01	.3510E-01	.4790E-02
.2005E 01	.6600E-01	.3821E-01	.2580E-02
.2106E 01	.6800E-01	.4564E-01	.3530E-02
.2212E 01	.6800E-01	.5506E-01	.2620E-02
.2293E 01	.6800E-01	.1003E 00	.3650E-01
.2414E 01	.7000E-01	.8395E-01	.8490E-02
.2505E 01	.1260E 00	.1103E 00	.9490E-02
.2615E 01	.7200E-01	.1063E 00	.4690E-02
.2712E 01	.7200E-01	.1414E 00	.1250E-01
.2813E 01	.7400E-01	.1555E 00	.9780E-02
.2924E 01	.7600E-01	.1835E 00	.1580E-01
.3015E 01	.7600E-01	.1745E 00	.7700E-02
.3118E 01	.7800E-01	.2056E 00	.1600E-01
.3215E 01	.8000E-01	.2347E 00	.1100E-01
.3313E 01	.8000E-01	.2337E 00	.1100E-01
.3415E 01	.8200E-01	.2457E 00	.1800E-01
.3616E 01	.8400E-01	.3159E 00	.1400E-01
.3623E 01	.2220E 00	.2899E 00	.1300E-01
.3711E 01	.8400E-01	.3220E 00	.1800E-01
.3807E 01	.8600E-01	.3510E 00	.2500E-01
.3906E 01	.8800E-01	.3611E 00	.1600E-01
.3960E 01	.1100E 00	.3250E 00	.1600E-01
.4008E 01	.8800E-01	.3591E 00	.2100E-01
.4161E 01	.1220E 00	.3400E 00	.1500E-01
.4117E 01	.9000E-01	.3631E 00	.1600E-01
.4215E 01	.9200E-01	.4012E 00	.3000E-01
.4319E 01	.9600E-01	.4112E 00	.1800E-01
.4359E 01	.1240E 00	.4022E 00	.1700E-01
.4421E 01	.9600E-01	.4202E 00	.1800E-01

TABLE IX (Cont'd)

E_n (MeV)	Resolution (MeV)	σ_{np} (barn)	$\pm \Delta\sigma_{np}$ (barn)
.4554E 01	.1240E 00	.4072E 00	.1700E-01
.4737E 01	.1560E 00	.4072E 00	.1800E-01
.4810E 01	.1180E 00	.4072E 00	.1800E-01
.4938E 01	.1760E 00	.4724E 00	.2000E-01
.5102E 01	.1220E 00	.4543E 00	.1900E-01
.5138E 01	.1560E 00	.4644E 00	.2000E-01
.5193E 01	.1260E 00	.4734E 00	.2300E-01
.5197E 01	.1240E 00	.4543E 00	.2000E-01
.5291E 01	.1260E 00	.5035E 00	.2500E-01
.5295E 01	.1240E 00	.5005E 00	.2300E-01
.5373E 01	.1620E 00	.5155E 00	.2500E-01
.5489E 01	.1300E 00	.5185E 00	.2500E-01
.5681E 01	.1320E 00	.5958E 00	.2900E-01
.5773E 01	.1620E 00	.6269E 00	.3000E-01
.5870E 01	.1660E 00	.5887E 00	.3300E-01
.5398E 01	.3300E 00	.4963E 00	.2482E-01
.5944E 01	.3240E 00	.5464E 00	.2732E-01
.6468E 01	.3300E 00	.5483E 00	.2742E-01
.6980E 01	.3400E 00	.5610E 00	.2805E-01
.7482E 01	.3520E 00	.5796E 00	.2956E-01
.7943E 01	.3680E 00	.5920E 00	.2960E-01
.8438E 01	.3840E 00	.5700E 00	.2850E-01
.8930E 01	.4020E 00	.5498E 00	.2804E-01
.9415E 01	.4220E 00	.5764E 00	.3055E-01
.9897E 01	.4420E 00	.5731E 00	.3095E-01

B. Fine resolution cross sections for E_n = 2.85 - 4.02 MeV:

E_n (MeV)	Resolution (MeV)	σ_{np} (barn)	$\pm \Delta\sigma_{np}$ (barn)
.2854E 01	.4200E-01	.1344E 00	.6500E-02
.2878E 01	.4200E-01	.1625E 00	.8000E-02
.2904E 01	.4200E-01	.1745E 00	.8000E-02
.2931E 01	.4200E-01	.1996E 00	.1000E-01
.2956E 01	.4200E-01	.2026E 00	.1000E-01
.2983E 01	.4200E-01	.2066E 00	.1000E-01
.3006E 01	.4200E-01	.1896E 00	.1000E-01
.3031E 01	.4200E-01	.1866E 00	.9000E-02
.3082E 01	.4400E-01	.1855E 00	.9000E-02
.3107E 01	.4400E-01	.1655E 00	.8000E-02
.3132E 01	.4400E-01	.1835E 00	.9000E-02
.3158E 01	.4400E-01	.2106E 00	.1000E-01
.3183E 01	.4400E-01	.2086E 00	.1000E-01
.3208E 01	.4400E-01	.2207E 00	.1100E-01
.3235E 01	.4400E-01	.2758E 00	.1400E-01

TABLE IX (Cont'd)

E_n (MeV)	Resolution (MeV)	σ_{np} (barn)	$\pm \Delta\sigma_{np}$ (barn)
.3261E 01	.4400E-01	.2387E 00	.1200E-01
.3286E 01	.4400E-01	.2327E 00	.1200E-01
.3312E 01	.4400E-01	.2217E 00	.1100E-01
.3336E 01	.4400E-01	.2156E 00	.1000E-01
.3361E 01	.4400E-01	.2317E 00	.1100E-01
.3378E 01	.4400E-01	.2287E 00	.1200E-01
.3411E 01	.4400E-01	.2427E 00	.1200E-01
.3438E 01	.4400E-01	.2337E 00	.1100E-01
.3464E 01	.4400E-01	.2668E 00	.1300E-01
.3488E 01	.4400E-01	.2738E 00	.1300E-01
.3514E 01	.4400E-01	.2828E 00	.1400E-01
.3540E 01	.4400E-01	.2768E 00	.1400E-01
.3564E 01	.4400E-01	.2969E 00	.1500E-01
.3595E 01	.4400E-01	.2788E 00	.1400E-01
.3614E 01	.4400E-01	.2959E 00	.1400E-01
.3641E 01	.4600E-01	.3019E 00	.1500E-01
.3666E 01	.4600E-01	.2828E 00	.1400E-01
.3691E 01	.4600E-01	.2989E 00	.1500E-01
.3717E 01	.4600E-01	.2989E 00	.1500E-01
.3741E 01	.4600E-01	.3129E 00	.1500E-01
.3766E 01	.4600E-01	.3109E 00	.1500E-01
.3793E 01	.4600E-01	.3199E 00	.1600E-01
.3817E 01	.4600E-01	.3079E 00	.1500E-01
.3842E 01	.4800E-01	.3551E 00	.1800E-01
.3867E 01	.4800E-01	.3751E 00	.1800E-01
.3894E 01	.4800E-01	.3320E 00	.1600E-01
.3918E 01	.4800E-01	.3470E 00	.1700E-01
.3943E 01	.4800E-01	.3470E 00	.1700E-01
.3969E 01	.4800E-01	.3811E 00	.1900E-01
.3994E 01	.4800E-01	.3500E 00	.1700E-01
.4019E 01	.4800E-01	.3370E 00	.1600E-01

TABLE X

Measured Cross Sections for the
$^{59}Co(n,p)^{59}Fe$ Reaction

E_n (MeV)	Resolution (MeV)	σ_{np} (barn)	$\pm \Delta\sigma$ (barn)
.4334E 01	.1580E 00	.6205E-02	.5150E-03
.4534E 01	.1580E 00	.6947E-02	.4793E-03
.4735E 01	.1600E 00	.8311E-02	.5735E-03
.4935E 01	.1600E 00	.7760E-02	.4889E-03
.5136E 01	.1620E 00	.1030E-01	.5459E-03
.5336E 01	.1640E 00	.1182E-01	.8038E-03
.5536E 01	.1640E 00	.1298E-01	.7658E-03
.5737E 01	.1660E 00	.1237E-01	.1089E-02
.5837E 01	.1680E 00	.1489E-01	.8487E-03
.5956E 01	.3260E 00	.1373E-01	.7002E-03
.6483E 01	.3360E 00	.1542E-01	.8635E-03
.6993E 01	.3540E 00	.1893E-01	.1098E-02
.7517E 01	.3700E 00	.2145E-01	.1158E-02
.8012E 01	.3860E 00	.2474E-01	.1336E-02
.8975E 01	.4260E 00	.2757E-01	.1516E-02
.9461E 01	.4480E 00	.3120E-01	.1810E-02
.9944E 01	.4700E 00	.3481E-01	.1984E-02

TABLE XI

Measured Cross Sections for the $^{64}Zn(n,p)^{64}Cu$ Reaction

E_n (MeV)	Resolution (MeV)	σ_{np} (barn)	$\pm \Delta\sigma_{np}$ (barn)
.1159E 01	.1020E 00	.2243E-03	.1750E-04
.1363E 01	.1040E 00	.4886E-03	.3127E-04
.1571E 01	.1020E 00	.1212E-02	.7999E-04
.1774E 01	.1020E 00	.2452E-02	.1398E-03
.1949E 01	.1600E 00	.5485E-02	.2852E-03
.2154E 01	.1580E 00	.1007E-01	.5136E-03
.2356E 01	.1580E 00	.1735E-01	.8849E-03
.2562E 01	.1560E 00	.2952E-01	.1506E-02
.2762E 01	.1560E 00	.4992E-01	.2496E-02
.2963E 01	.1560E 00	.7360E-01	.3680E-02
.3165E 01	.1560E 00	.9145E-01	.4573E-02
.3367E 01	.1560E 00	.1055E 00	.5275E-02
.3568E 01	.1560E 00	.1101E 00	.5505E-02
.3770E 01	.1560E 00	.1211E 00	.6055E-02
.3958E 01	.1560E 00	.1257E 00	.6285E-02
.4172E 01	.1580E 00	.1285E 00	.6425E-02
.4372E 01	.1580E 00	.1380E 00	.6900E-02
.4573E 01	.1600E 00	.1413E 00	.7065E-02
.4799E 01	.1620E 00	.1408E 00	.7040E-02
.4974E 01	.1620E 00	.1561E 00	.7805E-02
.5174E 01	.1640E 00	.1587E 00	.7935E-02
.5377E 01	.1660E 00	.1655E 00	.8275E-02
.5576E 01	.1660E 00	.1680E 00	.8400E-02
.5384E 01	.3340E 00	.1437E 00	.7185E-02
.5725E 01	.3280E 00	.1595E 00	.8135E-02
.6277E 01	.3260E 00	.1668E 00	.8507E-02
.6978E 01	.3340E 00	.1631E 00	.8155E-02
.7485E 01	.3500E 00	.1744E 00	.8720E-02
.7984E 01	.3640E 00	.1747E 00	.8910E-02
.8478E 01	.3820E 00	.1859E 00	.9480E-02
.8968E 01	.3980E 00	.1907E 00	.9726E-02
.9455E 01	.4180E 00	.1904E 00	.9900E-02
.9939E 01	.4360E 00	.1884E 00	.9985E-02

TABLE XII

Evaluated Cross Sections for the $^{27}Al(n,p)^{27}Mg$ Reaction

E_n (MeV)	σ_{np} (barn)	E_n (MeV)	σ_{np} (barn)	E_n (MeV)	σ_{np} (barn)	E_n (MeV)	σ_{np} (barn)
2.8	0.39×10^{-3}	3.78	0.0088	4.7	0.0185	5.625	0.046
2.95	0.82×10^{-3}	3.8	0.0073	4.74	0.0185	5.675	0.055
3.0	0.97×10^{-3}	3.84	0.0045	4.8	0.0135	5.71	0.068
3.05	0.00115	3.87	0.0044	4.83	0.0135	5.74	0.068
3.12	0.002	3.95	0.0069	4.9	0.019	5.8	0.0475
3.2	0.0021	4.0	0.0071	4.98	0.028	5.875	0.044
3.24	0.0026	4.05	0.0066	5.04	0.028	6.0	0.043
3.27	0.0026	4.11	0.0051	5.1	0.0263	6.25	0.044
3.3	0.00205	4.15	0.0051	5.15	0.029	6.5	0.046
3.34	0.00205	4.2	0.007	5.2	0.03	7.0	0.055
3.4	0.0038	4.25	0.009	5.25	0.028	7.5	0.064
3.46	0.0076	4.3	0.0115	5.28	0.026	8.0	0.072
3.5	0.0076	4.34	0.0115	5.33	0.026	8.5	0.078
3.54	0.0054	4.37	0.0108	5.37	0.0308	9.0	0.0815
3.57	0.0054	4.42	0.0108	5.42	0.0315	9.5	0.084
3.61	0.0069	4.45	0.012	5.45	0.0293	10.0	0.086
3.65	0.069	4.57	0.0195	5.47	0.0295		
3.68	0.0065	4.63	0.0197	5.5	0.035		
3.72	0.0065	4.65	0.0177	5.525	0.042		
3.75	0.0088	4.68	0.0175	5.575	0.044		

TABLE XIII

Evaluated Cross Sections for the $^{46}Ti(n,p)^{46}Sc$ Reaction

E_n (MeV)	σ_{np} (barn)	E_n (MeV)	σ_{np} (barn)
3.6	0.0125	6.0	0.118
3.9	0.019	6.5	0.143
4.0	0.023	7.0	0.167
4.2	0.032	7.5	0.19
4.3	0.037	8.0	0.207
4.5	0.045	8.5	0.219
4.7	0.057	9.0	0.226
5.0	0.072	9.5	0.232
5.2	0.08	10.0	0.234
5.5	0.094		

TABLE XIV

Evaluated Cross Sections for the $^{47}Ti(n,p)^{47}Sc$ Reaction

E_n (MeV)	σ_{np} (barn)	E_n (MeV)	σ_{np} (barn)	E_n (MeV)	σ_{np} (barn)
0.914	0.248×10^{-4}	2.33	0.032	4.6	0.074
1.13	0.00122	2.47	0.032	5.0	0.077
1.23	0.0029	2.6	0.0305	5.5	0.087
1.3	0.0032	2.7	0.0305	6.0	0.095
1.5	0.0039	2.9	0.035	6.5	0.1
1.6	0.0049	3.1	0.042	7.0	0.105
1.8	0.0087	3.3	0.049	8.0	0.119
2.0	0.0144	3.5	0.056	9.0	0.132
2.1	0.0175	3.8	0.062	10.0	0.141
2.2	0.021	4.0	0.066		
2.3	0.03	4.3	0.071		

TABLE XV

Evaluated Cross Sections for the $^{48}Ti(n,p)^{48}Sc$ Reaction

E_n (MeV)	σ_{np} (barn)	E_n (MeV)	σ_{np} (barn)
4.7	0.23×10^{-4}	5.9	0.148×10^{-2}
4.9	0.7×10^{-4}	6.0	0.18×10^{-2}
5.0	0.87×10^{-4}	6.2	0.24×10^{-2}
5.1	0.95×10^{-4}	6.5	0.37×10^{-2}
5.15	0.107×10^{-3}	7.0	0.65×10^{-2}
5.2	0.175×10^{-3}	7.5	0.01
5.24	0.25×10^{-3}	8.0	0.0133
5.3	0.31×10^{-3}	8.5	0.0164
5.5	0.48×10^{-3}	9.0	0.02
5.6	0.52×10^{-3}	9.5	0.0235
5.7	0.66×10^{-3}	10.0	0.028

TABLE XVI

Evaluated Cross Sections for the $^{54}Fe(n,p)^{54}Mn$ Reaction

E_n (MeV)	σ_{np} (barn)	E_n (MeV)	σ_{np} (barn)
2.0	0.014	3.9	0.263
2.2	0.025	4.1	0.28
2.4	0.046	4.5	0.334
2.6	0.075	5.0	0.4
2.7	0.095	5.3	0.432
2.8	0.114	5.6	0.455
3.0	0.132	6.1	0.468
3.2	0.156	6.5	0.47
3.4	0.2	7.0	0.47
3.5	0.23	8.5	0.465
3.6	0.242	10.0	0.46
3.7	0.25		

TABLE XVII

Evaluated Cross Sections for the $^{56}Fe(n,p)^{56}Mn$ Reaction

E_n (MeV)	σ_{np} (barn)	E_n (MeV)	σ_{np} (barn)
4.0	0.62×10^{-5}	5.5	0.47×10^{-2}
4.2	0.225×10^{-4}	5.75	0.0085
4.3	0.45×10^{-4}	6.0	0.0123
4.5	0.138×10^{-3}	6.5	0.02
4.7	0.365×10^{-3}	7.0	0.028
4.8	0.57×10^{-3}	7.5	0.035
4.9	0.75×10^{-3}	8.5	0.0475
5.0	0.95×10^{-3}	9.0	0.0536
5.2	0.18×10^{-2}	9.5	0.0586
5.4	0.335×10^{-2}	10.0	0.0625

TABLE XVIII

Evaluated Cross Sections for the $^{58}Ni(n,p)^{58}Co$ Reaction

E_n (MeV)	σ_{np} (barn)	E_n (MeV)	σ_{np} (barn)	E_n (MeV)	σ_{np} (barn)
0.57	0.2×10^{-5}	1.5	0.0134	3.75	0.327
0.62	0.7×10^{-5}	1.6	0.0166	4.0	0.354
0.68	0.2×10^{-4}	1.7	0.0225	4.25	0.386
0.7	0.36×10^{-4}	1.8	0.0285	4.5	0.41
0.74	0.9×10^{-4}	2.0	0.04	4.75	0.42
0.8	0.19×10^{-3}	2.2	0.054	5.0	0.44
0.86	0.3×10^{-3}	2.4	0.078	5.5	0.52
0.9	0.43×10^{-3}	2.5	0.094	5.75	0.548
1.0	0.9×10^{-3}	2.65	0.124	6.0	0.56
1.1	0.2×10^{-2}	2.85	0.162	7.0	0.57
1.16	0.35×10^{-2}	3.0	0.188	8.0	0.58
1.3	0.66×10^{-2}	3.25	0.23	9.0	0.57
1.4	0.0109	3.5	0.273	10.0	0.56

TABLE XIX

Evaluated Cross Sections for the $^{59}Co(n,p)^{59}Fe$ Reaction

E_n (MeV)	σ_{np} (barn)
4.3	0.0059
5.0	0.0094
5.5	0.0118
6.0	0.0143
6.5	0.0168
7.0	0.0193
7.5	0.0217
8.0	0.0242
8.5	0.0267
9.0	0.0291
9.5	0.0316
10.0	0.0341

TABLE XX

Evaluated Cross Sections for the $^{64}Zn(n,p)^{64}Cu$ Reaction

E_n (MeV)	σ_{np} (barn)	E_n (MeV)	σ_{np} (barn)
1.2	0.215×10^{-3}	3.75	0.12
1.4	0.58×10^{-3}	4.0	0.127
1.6	0.145×10^{-2}	4.5	0.138
1.8	0.31×10^{-2}	5.0	0.151
2.0	0.64×10^{-2}	5.25	0.159
2.3	0.015	5.5	0.162
2.5	0.026	6.0	0.164
2.7	0.043	7.0	0.168
2.8	0.054	7.5	0.172
2.9	0.065	8.0	0.179
3.0	0.075	8.5	0.185
3.25	0.097	9.0	0.188
3.5	0.11	10.0	0.191

FIGURE CAPTIONS

Fig. 1. Schematic diagram of apparatus used for fast-neutron irradiation of samples.

Figs.2-11. Measured cross sections for the $^{27}Al(n,p)^{27}Mg$, $^{46,47,48}Ti(n,p)^{46,47,48}Sc$, $^{54,56}Fe(n,p)^{54,56}Mn$, $^{58}Ni(n,p)^{58}Co$, $^{59}Co(n,p)^{59}Fe$ and $^{64}Zn(n,p)^{64}Cu$ reactions. Selected data sets from the literature are also plotted for comparison, when available.

Fig. 12. Evaluated cross sections for (n,p) reactions on ^{27}Al, $^{46,47,48}Ti$, $^{54,56}Fe$, ^{58}Ni, ^{59}Co and ^{64}Zn as well as for (n,f) reactions on $^{235,238}U$. Evaluated (n,p) cross sections are based entirely on the present work. Evaluated (n,f) cross reactions are derived from the ENDF/B-III data file (Ref. 16).

Fig. 1

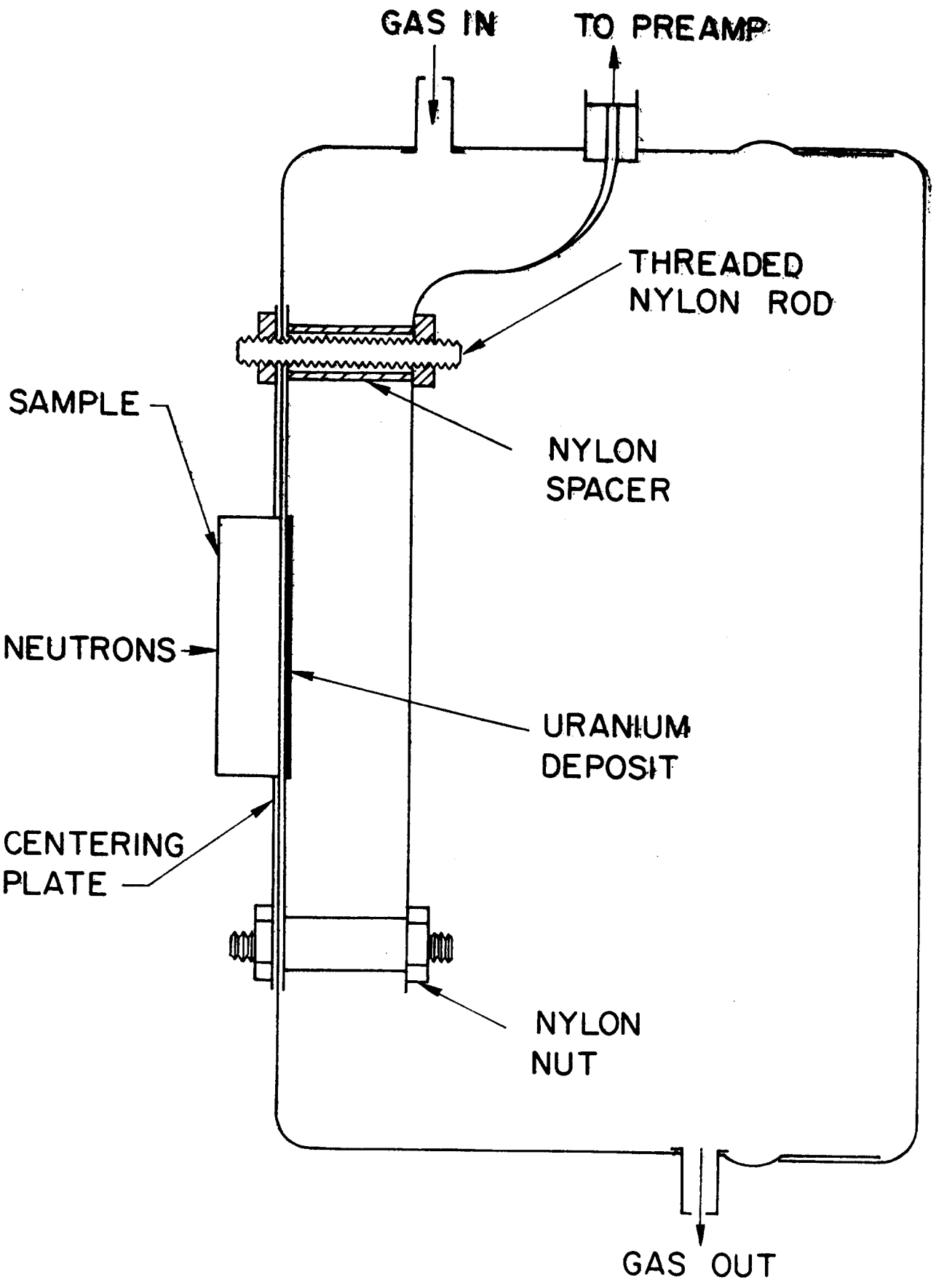
GAS IN
TO PREAMP
THREADED
NYLON ROD
SAMPLE
NYLON
SPACER
NEUTRONS
URANIUM
DEPOSIT
CENTERING
PLATE
NYLON
NUT
GAS OUT

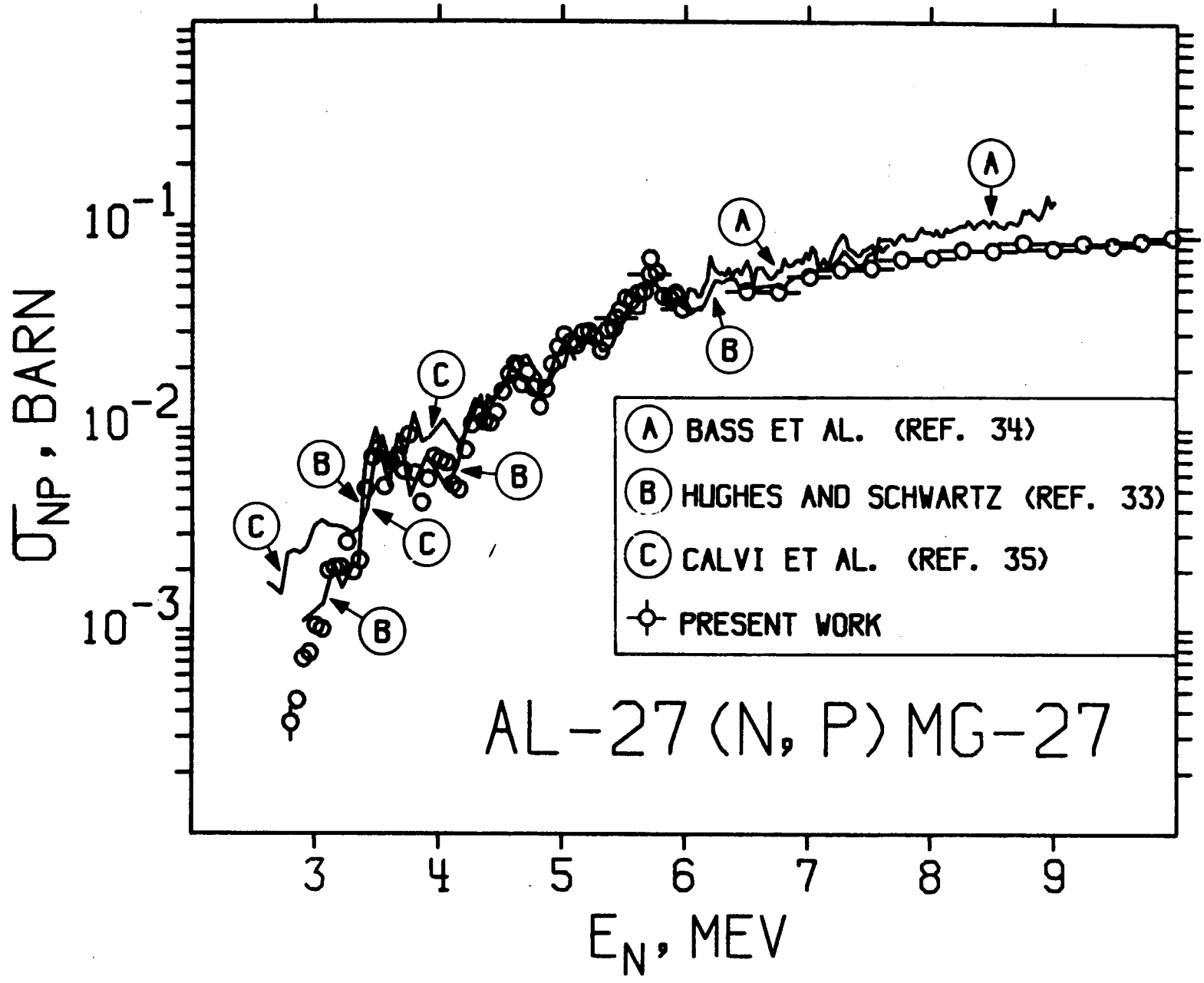
σ_{NP}, BARN
10^{-1}
10^{-2}
10^{-3}
3
4
5
6
7
8
9
E_N, MEV
A BASS ET AL. (REF. 34)
B HUGHES AND SCHWARTZ (REF. 33)
C CALVI ET AL. (REF. 35)
PRESENT WORK
AL-27 (N, P) MG-27

Fig. 2

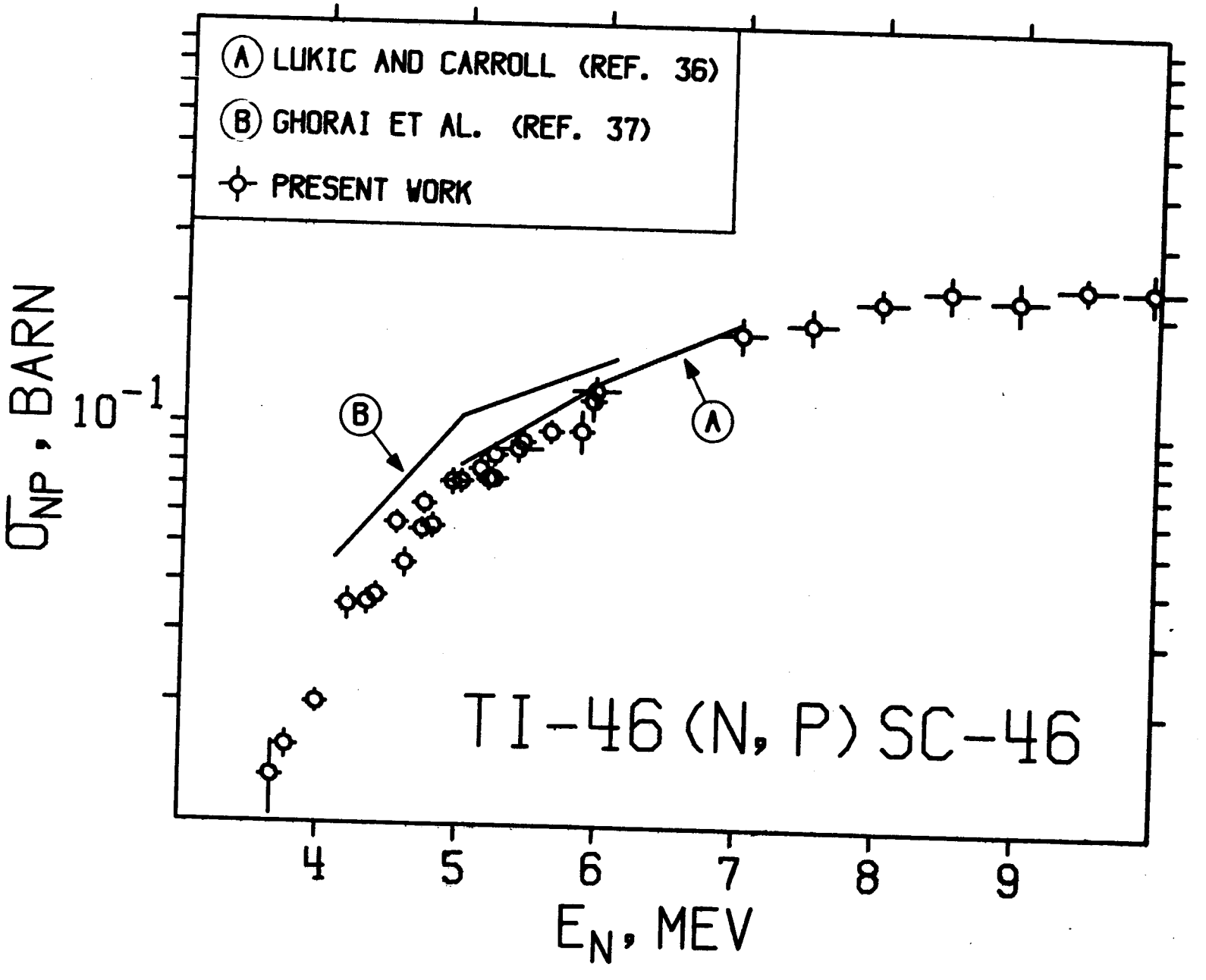
(A) LUKIC AND CARROLL (REF. 36)
(B) GHORAI ET AL. (REF. 37)
PRESENT WORK
σ_{NP}, BARN
10^{-1}
B
A
TI-46 (N, P) SC-46
4
5
6
7
8
9
E_N, MEV

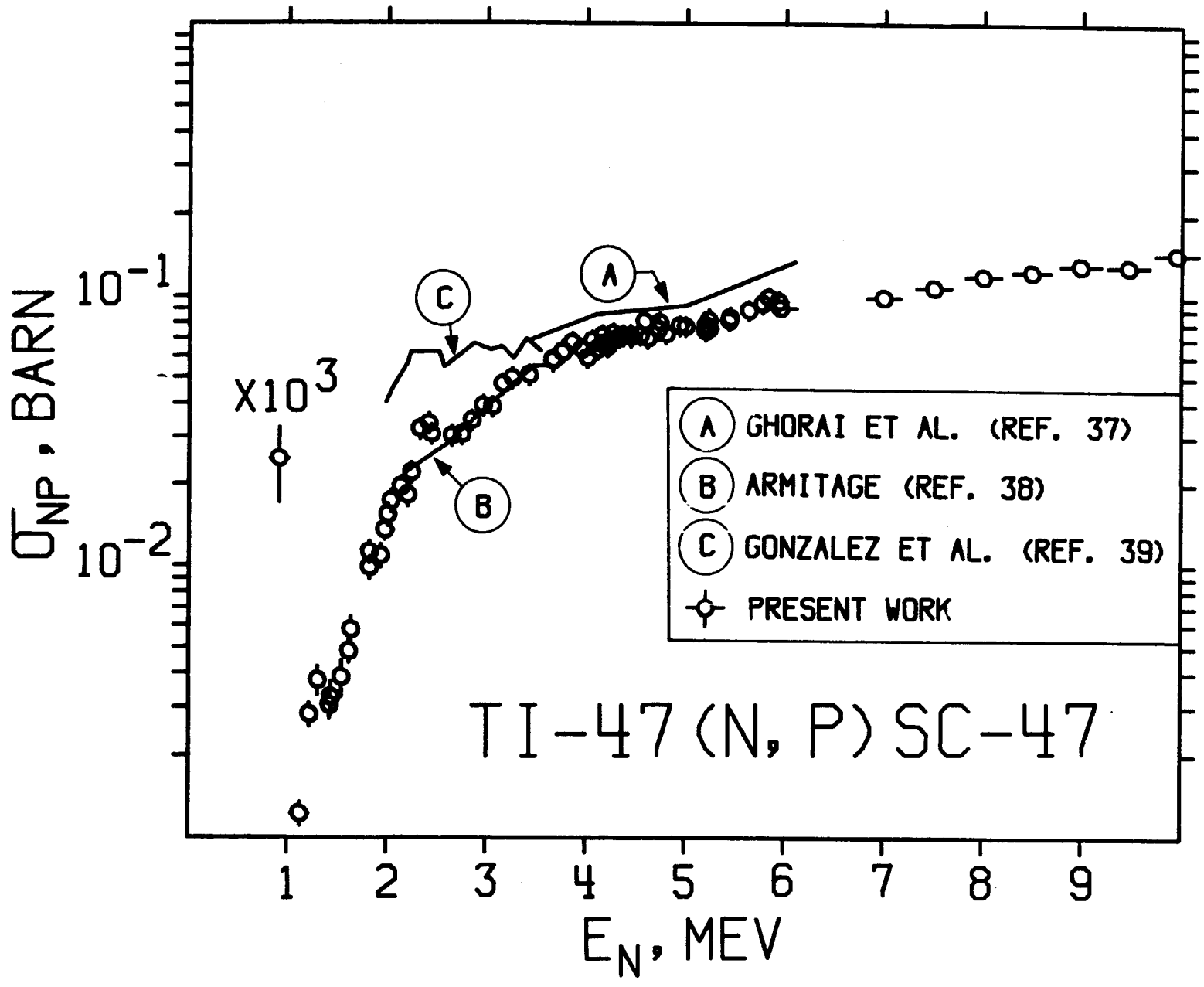
σ_{NP}, BARN
10^{-1}
10^{-2}
X10^3
A
B
C
A GHORAI ET AL. (REF. 37)
B ARMITAGE (REF. 38)
C GONZALEZ ET AL. (REF. 39)
PRESENT WORK
TI-47 (N, P) SC-47
1
2
3
4
5
6
7
8
9
E_N, MEV

Fig. 4

A LUKIC AND CARROLL (REF. 36)
PRESENT WORK
10^{-2}
10^{-3}
10^{-4}
σ_{NP}, BARN
A
TI-48 (N, P) SC-48
5
6
7
8
9
E_N, MEV

FIG. 5

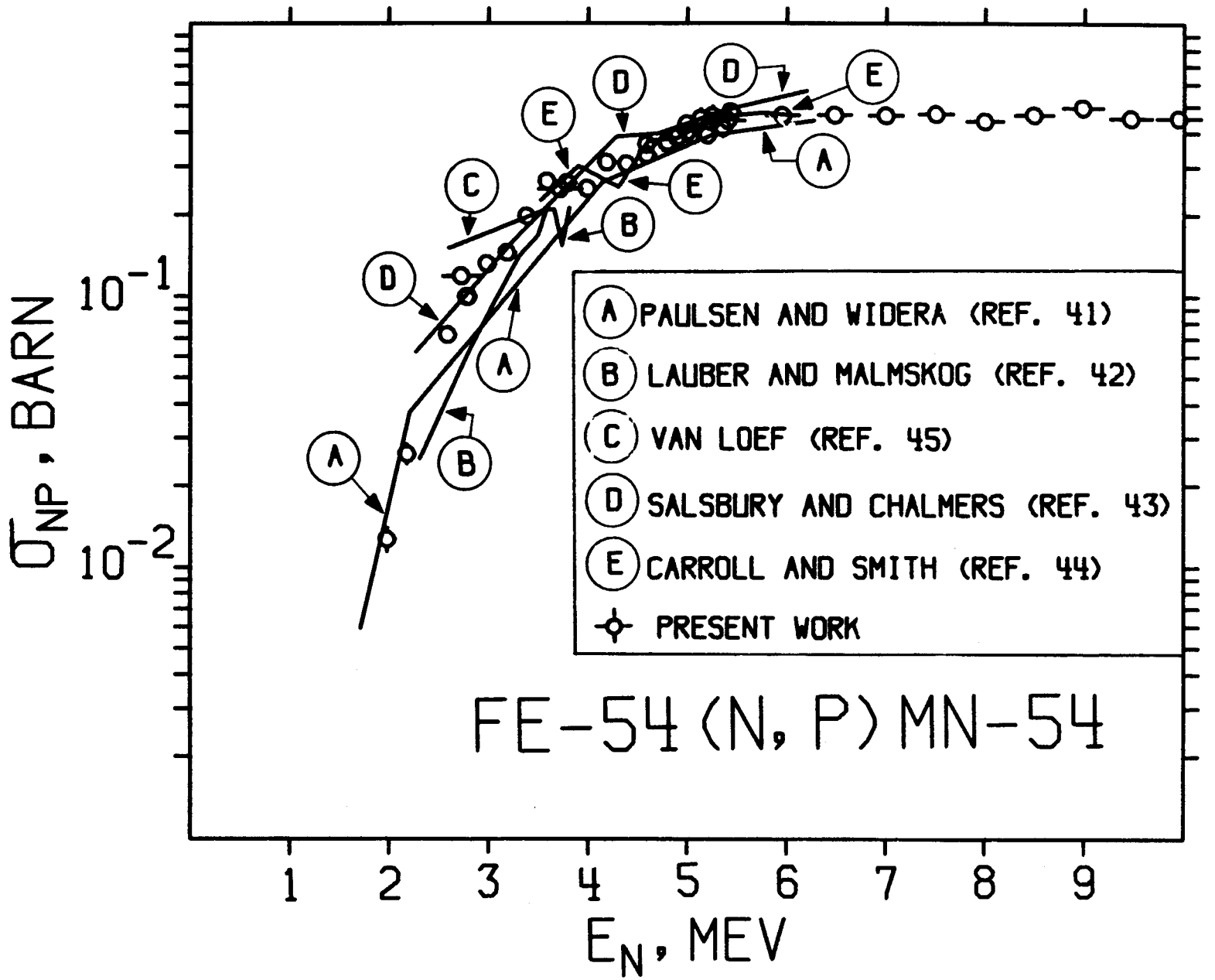
σ_{NP}, BARN
10^{-1}
10^{-2}
1
2
3
4
5
6
7
8
9
E_N, MEV
A PAULSEN AND WIDERA (REF. 41)
B LAUBER AND MALMSKOG (REF. 42)
C VAN LOEF (REF. 45)
D SALSBURY AND CHALMERS (REF. 43)
E CARROLL AND SMITH (REF. 44)
PRESENT WORK
FE-54 (N, P) MN-54

Fig. 6

Fig. 7

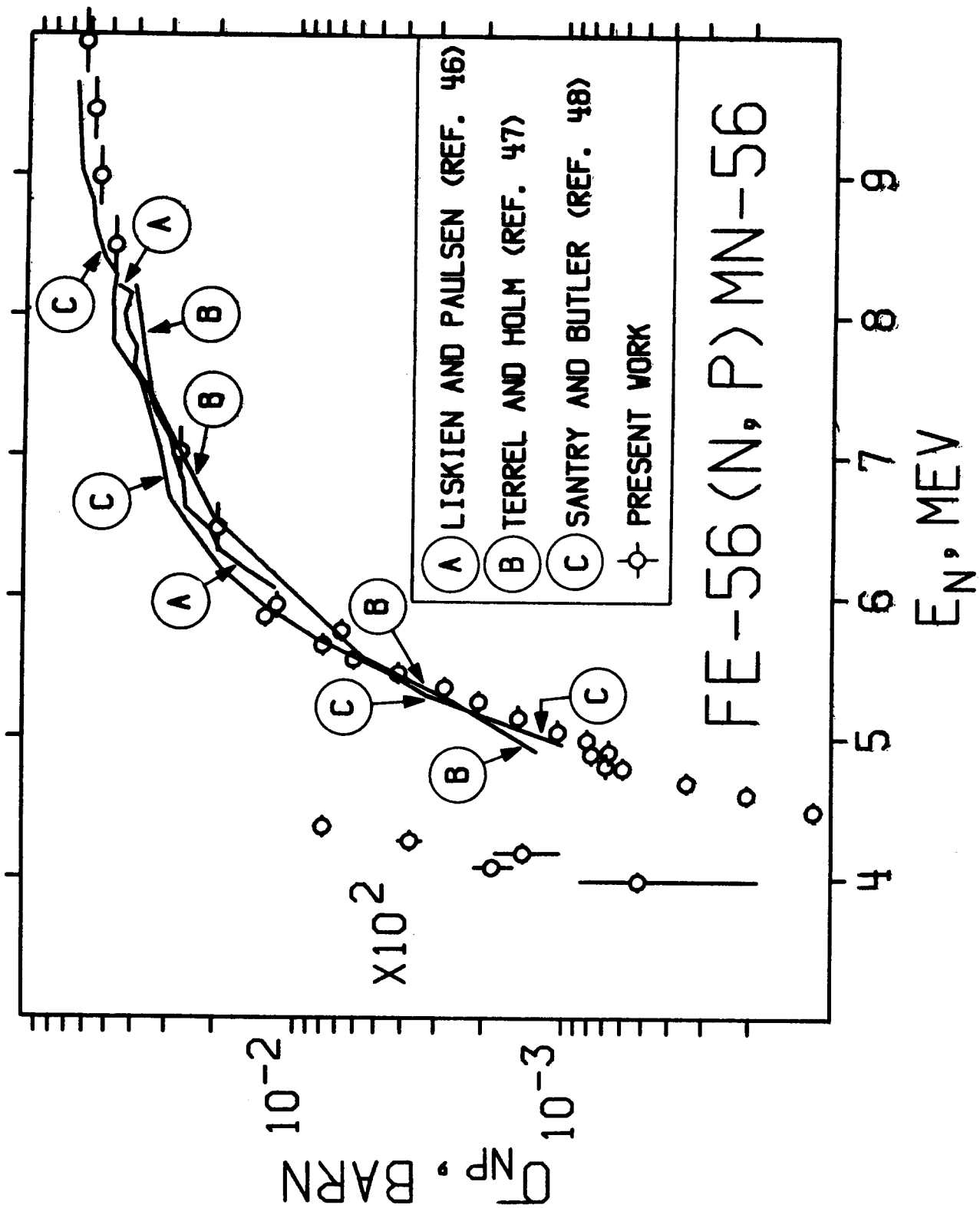
FE-56 (N, P) MN-56
A LISKIEN AND PAULSEN (REF. 46)
B TERREL AND HOLM (REF. 47)
C SANTRY AND BUTLER (REF. 48)
PRESENT WORK
σ_{Np}, BARN
10^{-2}
X10^{2}
10^{-3}
4
5
6
7
8
9
E_N, MEV

Fig. 8

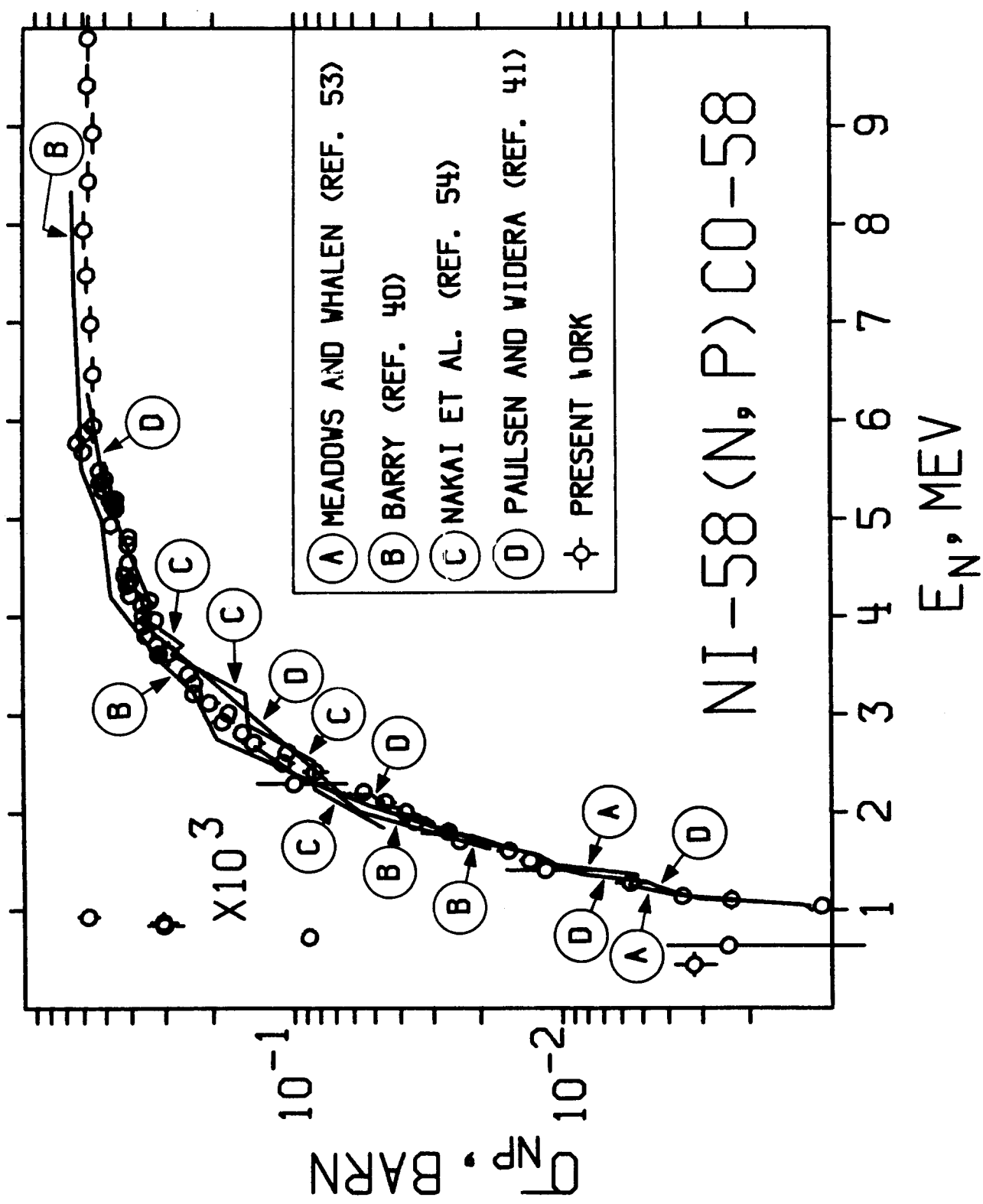
NI-58 (N, P) CO-58
A MEADOWS AND WHALEN (REF. 53)
B BARRY (REF. 40)
C NAKAI ET AL. (REF. 54)
D PAULSEN AND WIDERA (REF. 41)
PRESENT WORK
X10^3
10^-1
10^-2
σNp, BARN
EN', MEV
1
2
3
4
5
6
7
8
9

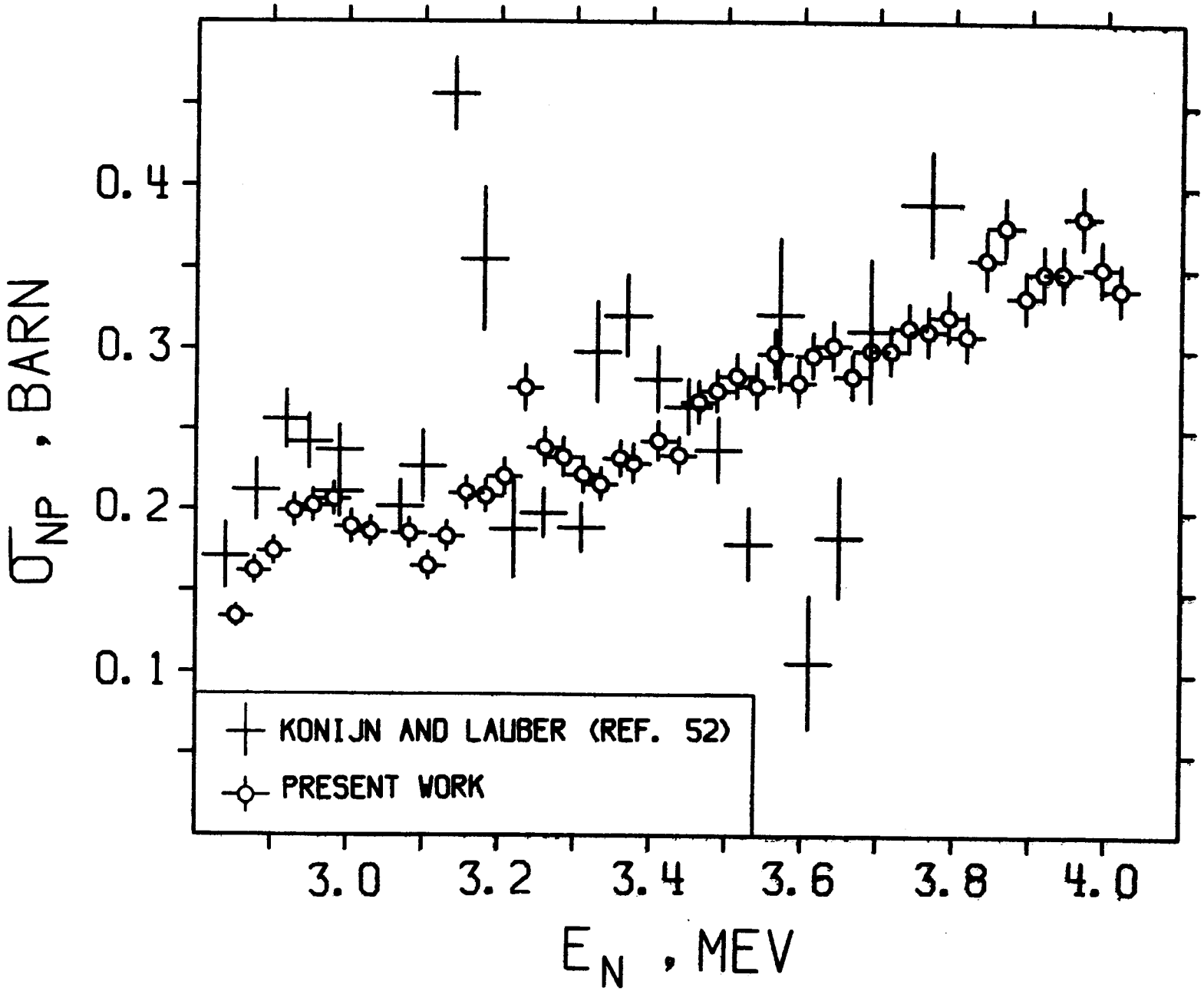
0.4
0.3
0.2
0.1
σ_{NP} , BARN
KONIJN AND LAUBER (REF. 52)
PRESENT WORK
3.0
3.2
3.4
3.6
3.8
4.0
E_N , MEV

Fig. 9

Fig. 10

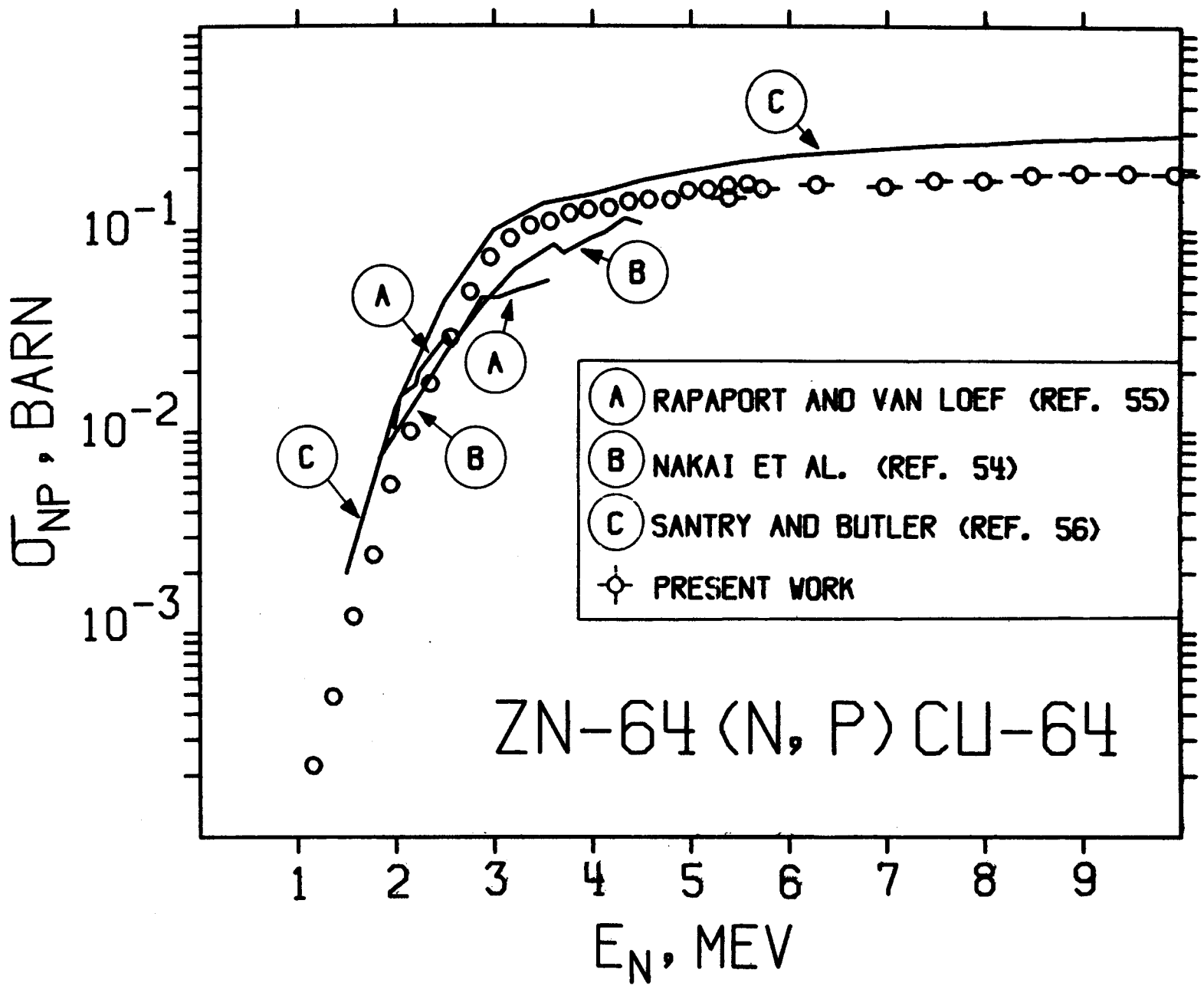
σ_{NP}, BARN
10^{-1}
10^{-2}
10^{-3}
1
2
3
4
5
6
7
8
9
E_N, MEV
A RAPAPORT AND VAN LOEF (REF. 55)
B NAKAI ET AL. (REF. 54)
C SANTRY AND BUTLER (REF. 56)
PRESENT WORK
ZN-64 (N, P) CU-64

Fig. 11

Fig. 12

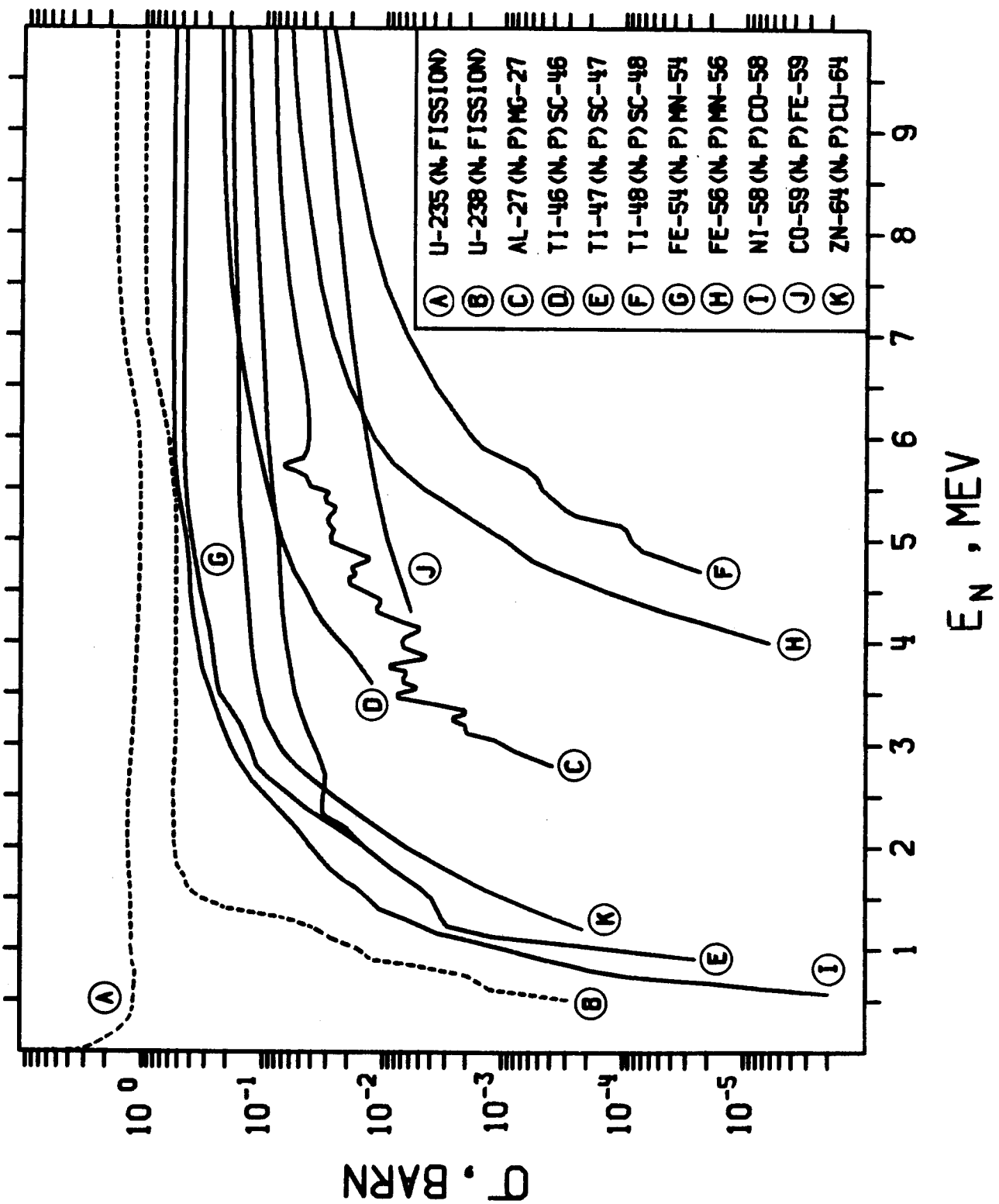
Ⓐ U-235 (N, FISSION)
Ⓑ U-238 (N, FISSION)
Ⓒ AL-27 (N, P) MG-27
Ⓓ TI-46 (N, P) SC-46
Ⓔ TI-47 (N, P) SC-47
Ⓕ TI-48 (N, P) SC-48
Ⓖ FE-54 (N, P) MN-54
Ⓗ FE-56 (N, P) MN-56
Ⓘ NI-58 (N, P) CO-58
Ⓙ CO-59 (N, P) FE-59
Ⓚ ZN-64 (N, P) CU-64
σ, BARN
10^{0}
10^{-1}
10^{-2}
10^{-3}
10^{-4}
10^{-5}
1
2
3
4
5
6
7
8
9
E_N, MEV